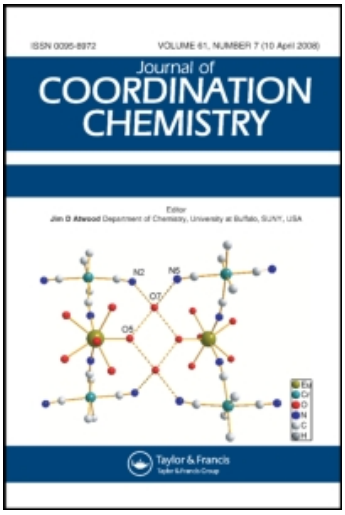

Journal of Coordination Chemistry
Publication details, including instructions for authors and subscription information:
http://www.informaworld.com/smpp/title~content=t713455674

REVIEW: THE CONCEPT OF VIBRONIC INTERACTIONS IN CRYSTAL STEREOCHEMISTRY OF TRANSITION METAL COMPOUNDS

Isaac B. Bersuker[a]
[a] Department of Chemistry and Biochemistry and College of Pharmacy, The University of Texas at Austin, Austin, Texas, USA

To cite this Article Bersuker, Isaac B.(1995) 'REVIEW: THE CONCEPT OF VIBRONIC INTERACTIONS IN CRYSTAL STEREOCHEMISTRY OF TRANSITION METAL COMPOUNDS', Journal of Coordination Chemistry, 34: 4, 289 — 338
To link to this Article: DOI: 10.1080/00958979508024320
URL: http://dx.doi.org/10.1080/00958979508024320

J. Coord. Chem., 1995, Vol 34, pp. 289–338
Reprints available directly from the publisher
Photocopying permitted by license only

REVIEW

THE CONCEPT OF VIBRONIC INTERACTIONS IN CRYSTAL STEREOCHEMISTRY OF TRANSITION METAL COMPOUNDS

ISAAC B. BERSUKER

Department of Chemistry and Biochemistry and College of Pharmacy, The University of Texas at Austin, Austin, Texas 78712, USA

A review of recent achievements in the application of the theory of vibronic coupling to stereochemical problems of transition metal compounds is given. After the formulation of the concept of vibronic interactions relevant to stereochemistry, its general validity is discussed, and it is shown that in the crystal state long-range forces alone cannot produce distortions of high-symmetry lattice configurations. The latter may become unstable due to the vibronic coupling which is of local origin. For ferroelectric distortions in perovskite-type crystals this result is confirmed by quite a number of different experimental data; it casts heavy doubts on the very existence of displacive phase transitions. Among other stereochemical problems solved by means of the vibronic approach, the following are briefly considered: local distortions produced by *d* electrons using the $CuCl_5^{3-}$ vs $ZnCl_5^{3-}$ polyhedra in similar crystals; crystal implications in the effects of plasticity, distortion isomers, and temperature-dependent solid-state conformers; a general solution for the origin of active and inert $(ns)^2$ lone pairs; and the vibronic treatment of the problem of mutual influence of ligands in complexes of transition and post-transition elements. Taken as a whole, the vibronic approach can be regarded as a further step in theoretical developments of transition metal stereochemistry.

KEYWORDS: stereochemistry, vibronic interactions, crystal chemistry, transition metal compounds displacive phase transitions

CONTENTS

1. INTRODUCTION

Stereochemistry underlies chemical intelligence; without the assumption of molecular shapes there is no way to rationalize molecular structures and chemical transformations. This is why the origin of stereochemistry is given much attention, especially in the last two decades (see, e.g.,[1-10] and references therein).

On the other hand, from the quantum-chemical point of view, the basic definition of molecular shapes is not trivial. The belief that any stable polyatomic system has some fixed geometrical arrangement in space is, in fact, based on the *adiabatic approximation*; i.e., on the assumption that there are fast electrons and slow nuclei, the latter moving in the time-averaged field of the former. If the adiabatic potential (the potential energy of the nuclei in the mean field of the electrons) has a minimum and the nuclei perform small vibrations at the minimum point, *the coordinates of this minimum point may be assumed to describe the molecular shape.*

The adiabatic approximation works well in the majority of cases but not always: there are quite a number of situations when it fails and hence the notion of molecular shape becomes uncertain (note that, strictly speaking, the nuclei should be described by wavefunctions, not coordinates). In particular, this may happen to any system in nuclear configurations with degenerate or pseudodegenerate electronic states, since in these states the adiabatic potential has no minima. As a consequence, it may have two or several or an infinite number of minima (a trough) at other configurations with lower symmetry. In these cases the molecular system, instead of small vibrations, performs large-amplitude hindered motions, free (internal) rotations, conformational structural changes, etc. These situations are usually termed as non-rigid molecular systems, Jahn-Teller and *pseudo* Jahn-Teller effects, Berry rotations, structural phase transitions or conformational flexibility.[1,2,8,10]

If the adiabatic potential has a minimum and hence the molecular system has a well defined molecular shape, the latter can be found (at least in principle) by means of electronic structure calculations with geometry optimization. However, the results of electronic structure computations are numerical, and they characterize the specific system for which the calculations were carried out. The computer evaluation of the possible geometry of the system (as well as its energy spectrum and wavefunctions) is most important to the theory of electronic structure of matter, but it gives no direct indication of the origin of the results. The computer output does not answer the question of why the system under consideration should have the specific properties that emerge from the computations, and therefore the data obtained are not directly transferable to other molecular systems. From this point of view computer results may be regarded as an output of a *computer experiment.*

To construct the theory of molecular structure, numerical data on the electronic structure and geometry of series of molecular systems obtained from different experimental sources, including computer experiments, should be generalized and rationalized in terms of *analytical models.* The latter seem to be inevitable in any theoretical generalization. For coupling between the electronic motion and the nuclear framework and its dynamics, which is most important to all the molecular properties, including molecular shapes, such a model is provided by the concept of vibronic interactions based on *the theory of vibronic coupling.*[8,11-14] The theory began from a rather limited field of electron-vibrational interactions in orbitally degenerate electronic states that result in the Jahn-Teller effect. It has been initially

aimed at considering the cases of non-trivial molecular shapes, mentioned above, when there is more than one minimum of the adiabatic potential and complicated nuclear dynamics. These cases, even now, cannot be handled directly by just electronic structure calculations and geometry optimization.

In the past decades the vibronic theory expanded significantly. Presently the concept of vibronic interactions is, in principle, applicable to any polyatomic system. Although the importance of the vibronic effects varies from one system to another, there are no *a priori* exceptions to the applicability of this approach. In fact, the vibronic coupling theory is now a general tool to a more detailed understanding of *how electrons control molecular configurations* and relevant properties.

Another problem beyond the present abilities of electronic structure calculations is the role of the crystal lattice formation in local stereochemistry, i.e., the measure of participation of the lattice (long-range) forces in the local stereochemistry controlled mainly by short-range (chemical) forces. This problem is of special importance to transition metal coordination compounds which in most cases are stable in the crystalline state. It is an advantage of the vibronic approach that it allows us to consider both the long-range and short-range forces in the crystal and to reveal their relative contribution to the stereochemistry.

Irrelevant to electronic structure calculations and the vibronic coupling approach, the theory of stereochemistry of transition metal compounds has a long history.[3-7] The earlier models for transition metal crystal lattice formation have been mostly classical (ion ball packing). They were followed by more sophisticated semiclassical models based on 'charge packing', assuming some simplified charge distributions as packing elements. In more recent approaches the main idea is to take into account that, according to quantum-mechanics, the electronic charge distribution in atoms and molecules is non-totally symmetric. In this way the notions of directed valences and localized electronic pairs have been introduced, based on which model of valence shell electron pair repulsion (VSEPR) has been worked out.[3] In the VSEPR model, the molecular shape is determined by deviations from the high-symmetry configuration produced by the additional repulsion between the electronic pairs, including lone pairs. This approach has been continuously improved to estimate the repulsions by means of empirical coefficients and to evaluate the molecular shape from the condition of energy minimum.[7]

An attempt to overcome the restrictions of the semiclassical treatment of electrostatic charge interactions, but to preserve its simplicity, has been made based on the correspondence between lone pairs and non-bonding MO's.[15] This allowed for a more accurate formulation of the main conclusion of the VSEPR model. In the MO formulation it states that *the ligands are always located on the nodal lines, planes or cones of occupied non-bonding orbitals.* Further development of this approach resulted in the so-called complimentary spherical electron density model.[16] It explains, in particular, the origin of the inert gas rule which states that coordination systems and main group molecules with the valence electron configuration of the appropriate inert gas are most stable.

All these models are rather useful and contribute to the understanding of the origin of molecular shapes, but in essence they do not go beyond the idea of charge packing (optimal arrangement of charges compatible with their interaction) with more or less simplified presentation of the charge distribution by electronic pairs or non-bonding orbitals. A more rigorous quantum-mechanical treatment shows that,

strictly speaking, the semiclassical models based on VSEPR in application to transition metal coordination compounds may be inadequate. The main reason is that the electronic structure of such compounds, in general, cannot be described by localized electronic pairs because the metal-ligand bonds are essentially delocalized around the metal center (in three dimensions) due to the *d* electron participation.[10] For delocalized distributions the very idea of charge packing loses its physical sense. Besides, the low-in-energy excited electronic states that originate from the open *d*-electron shell strongly influence the stereochemistry;[8–10] these effects are almost completely out of consideration in semiclassical models. Note that the crystal aspects of the problem also escape attention in these models.

The main goal of the present paper is to give an account of the latest achievements in the development of the concept of vibronic interactions relevant to stereochemistry, to demonstrate its general validity as a tool to a better understanding of the origin of molecular shapes and crystal structures, and to reveal the role of electrons in local stereochemistry and crystal lattice formation for transition metal compounds. The formulation of the concept of vibronic interactions relevant to stereochemistry is briefly outlined in the next section followed by a general discussion of the relationship between the crystal factor and local (chemical) forces in the formation of the lattice (Section 3). This problem is elucidated in more detail by considering the origin of ferroelectricity in perovskite-type crystals taken as an example (Section 4). Important by themselves, the results obtained for this class of crystals have a more general meaning since they show explicitly that the so-called *displacive phase transitions may not exist:* they are of order-disorder nature.

Section 5 considers local distortions in transition metal coordination compounds that are controlled by *d* electrons *via* vibronic coupling. Here, again, the crystalline aspect of the problem may be very important in a series of new effects, some of which, plasticity, distortion isomers, and temperature dependent conformers, are discused (Section 6). A general formulation of the origin of active and inert $(ns)^2$ lone pairs is given in Section 7. The vibronic treatment of mutual influence of ligands in complexes of transition the post-transition elements is outlined briefly in Section 8, followed by Section 9, concluding remarks.

Taken as a whole, the vibronic approach can be regarded as a further step in theoretical development of transition metal stereochemistry.

2. FORMULATION OF THE CONCEPT OF VIBRONIC INTERACTIONS RELEVANT TO STEREOCHEMISTRY

The brief formulation of the concept of vibronic interactions is as follows. For any molecular system we can assume a specific geometric configuration, usually the high-symmetry configuration termed as the *reference configuration,* for which the energies of the ground and excited electronic states, E_0, E_1, and their wavefunctions $|0>$, $|1>$, are defined. Under nuclear displacements Q that lower the symmetry of the system, some of the electronic states of the reference configuration are no longer relevant to the system as separate ground and excited states because they become mixed. Using symmetrized coordinates $Q\alpha$ and denoting the reference configuration by $Q\alpha = 0$, we may expand the electron-nuclear and nuclear-nuclear interaction V(r,Q) with respect to small displacements $Q\alpha$:

$$V(r,Q) = V(r,0) + (1/2)\Sigma\alpha(\partial V/\partial Q\alpha)Q\alpha + \ldots \quad (1)$$

the full Hamiltonian being $H = Hr + V(r,Q)$ (r is the set of electronic variables). The electronic states of the reference configuration, defined above, are solutions of the Schrodinger equation with the Hamiltonian H that includes the first term V(r,0) only of the expansion (1). When the second, third, *etc.*, terms (the *vibronic interaction terms)* are taken into account, some or all of these electronic states mix (*vibronic mixing*).

In general, vibronic mixing of electronic states under nuclear displacements is rather common, until it becomes sufficiently strong and/or the mixing states are degenerate or close in energy (pseudodegenerate). In these cases the vibronic coupling results in a series of new effects and laws that control the properties of polyatomic systems; their investigation now forms a whole field in physics and chemistry of molecules and crystals which can be considered as based on *the concept of vibronic interactions.*[8,10,11,14]

If the ground state is degenerate, there are always such displacements $Q\alpha$ with respect to which, according to the Jahn-Teller theorem,[13] the system is unstable. With non-degenerate ground states, a similar instability may occur provided a certain relationship holds between the parameters of the ground and excited states and their vibronic coupling. If only one excited state satisfies the selection rules, outlined below, the resulting two-level problem of instability coincides with that of the *pseudo Jahn-Teller effect.*[8] The condition of instability of the reference configuration with respect to some $Q\alpha$ displacements is:

$$K_0\alpha < |F\alpha^{(01)}|^2/\Delta_{01} \quad (2)$$

where F is the *vibronic coupling constant,*

$$F\alpha^{(01)} = \langle 0|(\partial H/\partial Q\alpha)_0|1\rangle \quad (3)$$

$K_0{}^\alpha = M\omega^2$ is the *bare force constant* (i.e., the force constant calculated without taking into account the vibronic mixing):

$$K_0{}^\alpha = \langle 0|\ \partial^2 H/\partial Q\alpha^2)|0\rangle \quad (4)$$

$$2\Delta_{01} = E_1 - E_0 \quad (5)$$

is the energy gap between the ground and excited states, obtained with the zeroth order term in (1). By solving the secular equation for the vibronic mixing of these electronic states with the vibronic interaction terms in (1) considered as a perturbation, one can evaluate the adiabatic potential of the system in the space of $Q\alpha$ displacements.

In the case of many excited states $|i\rangle$ involved, their effect on the instability is additive; it can be termed the *multilevel pseudo Jahn-Teller effect.*[10] The condition of instability in this case is:

$$K_0{}^\alpha < \Sigma_i |F_\alpha{}^{(0i)}|^2/\Delta_{0i} \quad (6)$$

This formula emerges also from the general expression for the curvature K^α of the adiabatic potential in the $Q\alpha$ direction derived by means of second order perturbation theory:[17]

$$K\alpha = K_0{}^\alpha - \Sigma i |F\alpha^{(0i)}|^2/\Delta_{0i} \quad (7)$$

Eq. (3) imposes strong symmetry restrictions (selection rules) on the possible excited states which contribute to the instability of the system in the ground state: for nonzero values of the vibronic constant the product of symmetry representations of $|0>$, $|1>$, and $Q\alpha$ must contain the unit representation. For higher excited states Δ_{0i} is large thus reducing their contribution. Usually only one or several excited states contribute significantly to the instability of the polyatomic system (Section 5).

If the system is, in general, stable, the minima of the adiabatic potential correspond to distorted configurations. There are two or several or an infinite number of such equivalent distorted configurations; they are complimentary to each other in the sense that together they preserve the initial high symmetry of the reference system.

An interesting achievement in this field during the last decade was the proof that *the vibronic mixing of electronic states is the only possible source of molecular high-symmetry configuration instability.* Eq. (7) for the curvature of the adiabatic potential in the direction $Q\alpha$ can be presented as follows (for simplicity, the index α is omitted):

$$K = K_0 + K_v \tag{8}$$

where K_0 is the non-vibronic contribution to K given by Eq. (4), and

$$Kv = -\Sigma_i |F^{(0i)}|2/\Delta_{0i} \tag{9}$$

is the contribution of the vibronic coupling to the excited states. The vibronic part K_v is always negative thus lowering the curvature of the system in the ground state along the corresponding direction. If $|K_v| < K_0$, i.e., the inequality (6) holds, then the curvature K becomes negative and the reference configuration of the system is unstable with respect to the nuclear displacements under consideration. Such a possibility has been first analyzed by Bader[17] and discussed in more detail with examples by Pearson.[18]

However, the non-vibronic part of the curvature, the K_0 value itself may be negative, and then the reference configuration is unstable irrelevant to vibronic mixing. The question is thus whether it is possible that $K_0 < 0$. In the opposite case, i.e., if we can prove that $K_0 > 0$ for all cases, than the inequality (6) remains the only possibility for negative curvature and configuration instability. The recent achievement in this field, as mentioned above, is that the non-vibronic contribution to the adiabatic potential curvature of the high-symmetry reference configuration (i.e., in a configuration with $<0|\partial H/\partial Q|0> = 0$) K_0 in any direction Q is positive:

$$K_0 \geq 0 \tag{10}$$

This means that any high-symmetry molecular configuration is stable as long as the expectation value of the operator of curvature $\partial^2 H/\partial Q^2$ is calculated with the ground state wavefunction only, without involving vibronic mixing with excited states. The only possible reason for instability of the reference configuration is thus the vibronic contribution, i.e., the strong pseudo Jahn-Teller effect produced by vibronic mixing with the appropriate excited states expressed by inequality (6). The formulation of this statement and approximate proof has been given[19] followed by more rigorous treatments and analytical proofs.[12,20–22]

The physical meaning of the conclusion $K_0 \geq 0$ can be further explored by considering the terms K_0 and K_v after (4) and (9) in more detail. The matrix

element $<0|(\partial^2 H/\partial Q^2)_0|0>$ is determined by the ground state wavefunctions obtained with the nuclei fixed at the reference configuration. Hence

$$K_0 = (\partial^2 < 0|H|0 >/\partial Q^2)_0 = (\partial^2 E_0/\partial Q^2)_0 \tag{11}$$

where

$$E_0(Q) = <0|\ H\ |0> \tag{12}$$

is the total energy of the system as a function of nuclear coordinates calculated with ground state wavefunctions at fixed nuclei. Therefore $K_0 \geq 0$ means that if one does not allow the wavefunctions to change by nuclear displacements, to 'relax', the system cannot be unstable. In other words, if the electronic cloud obtained as an exact solution of the Schrodinger equation for the reference configuration is kept frozen, this configuration cannot be unstable. The vibronic term K_v in Eq. (9) just takes into account the 'relaxation' of the wavefunction when the nuclei displace *i.e.*, it allows for the electronic cloud to partially follow the nuclei in their displacements, and this effect is the only possibility to obtain the inequality $K < 0$ and instability of the reference configuration.

Note that the inner electrons which almost completely follow their nuclei can be included in the effective charge of the latter (the proof of $K_0 \geq 0$ does not depend on the nuclear charges). All electrons cannot be included since the valence electrons are (fully or partially) shared by near neighbor ions, and therefore they cannot follow completely neither of them (the near-neighbor ions may move in diferent directions).

For a further understanding of the origin of the vibronic instability the terms in the sum K_v after (9) may be divided into two groups:

(i) The basis wavefunctions $|0>$ and $|i>$ in the matrix element $F^{(0i)}$ are mainly from the same atom. In this case the term $|F^{(0i)}|^2/\Delta_{0i}$ can be interpreted as the contribution of the polarization of this atom by the corresponding displacements Q.

For instance, for the instability of the central position of the Ti ion in the octahedron of oxygens in the TiO_6^{8-} cluster of $BaTiO_3$ with respect to off-center displacements[23-25] (to be discussed in the next section), the contribution of the polarization of the oxygen atom by the off-center displacement of the titanium ion is given by the mixing of the oxygen $2p$ and $3s$ atomic function under this displacement:[25]

$$K_v^{pol} = -|< 2p_{\sigma z}(O)|(\partial V/\partial Q_z)_0|3_s(O) >|^2/\Delta_{2p3s} \tag{13}$$

Since the integrals $F^{(0i)} = < 0|(\partial V/\partial Q)_0|i>$ are calculated with the orthogonal (ground and excited) wavefunctions of the same atom, then transforming the symmetrized coordinate Q into Cartesian coordinates, and taking the corresponding derivative of the Coulomb potential $V = e^2|\mathbf{r} - \mathbf{R}\alpha|^{-1}$, we come to integrals of the type $I_x = < 0|(x\text{-}X\alpha)/|\mathbf{r} - \mathbf{R}\alpha|^3|i>$, where x are the electronic coordinates of the polarizing atom and $X\alpha$ are the nuclear coordinates of the displacing atoms. If we assume that $R\alpha$ is much larger than the atomic size (which is already true for the second coordination sphere), then $I_x \approx R\alpha^{-3} <0|\ x\ |i>$, and the polarization contribution is:

$$K_v^{pol} \approx e^2\alpha_x/R\alpha^{-6} \tag{14}$$

where, according to quantum mechanics,

$$\alpha_x = e^2|< 0| \times |i >|^2/\Delta oi \qquad (15)$$

is the part of the atomic polarizability in the x direction which is due to the contribution of the i-th excited state (the summation over i gives the full atomic polarizability in this direction).

(ii) The two functions in $F^{(oi)}$ are from two different (near-neighbor) atoms. In this case the vibronic contribution is due to new covalency produced by the distortion. Indeed, in the reference configuration the overlap of these two electronic states is zero (they are orthogonal), hence their vibronic mixing means that a non-zero overlap occurs under the low-symmetry displacements Q.

For the Ti ion off-cemter displacements with respect to the oxygen octahedron, mentioned above, the covalent contribution is due to the new overlap of the ground state t_{1u}-combination of the highest occupied $2p_{\pi z}$ functions of the oxygen atoms with the lowest unoccupied d_{xz} function of the titanium ion:[23-25]

$$K_v^{cov} = -< 2p_{\pi z}(O)|(\partial V/\partial Q_x)_0|3d_{xz}(Ti) >|^2/\Delta_{2p3d} \qquad (16)$$

The new overlap (which is forbidden by symmetry in the reference configuration) produces new (additional) covalency. The inequality (6), made possible by this term, means that with the new covalency the energy is lower than that of the reference configuration, resulting in instability.

Both kinds of vibronic contribution to instability, new covalency and atomic polarization, may be significant, but the numerical calculations performed so far show that the covalency contribution is an order of magnitude larger than the polarization. Table 1 shows three examples of such calculations:[26] the instability of NH_3 in the planar configuration with respect to out-of-plan displacements of the nitrogen atom (toward the stable C_{3v} configuration);[20] $CuCl_5^{3-}$ in the trigonal-bipyramidal configuration with respect to E′ displacements (toward a square pyramid)[27]; and the TiO_6^{8-} cluster in $BaTiO_3$ with respect to T_{1u} (Ti off-center) displacements initiating the spontaneous polarization of the crystal.[23-25,28] In all these examples the new covalency contribution to the instability is indeed much more significant, by at least an order of magnitude.

The proof of the uniqueness of the vibronic origin of configuration instability leads to some interesting direct consequences. Apart from the Bader-Pearson

Table 1 New covalency K_v^{cov} vs. polarization K_v^{pol} contributions to the instability of the high-symmetry configuration of several molecular systems (arrow indicates one-electron excitation).

Instability parameters	NH_3	$CuCl_5^{3-}$	TiO_6 in $BaTiO_3$
Reference configuration	Planar D_{3h}	Trigonal bipyramidal D_{3h}	Octahedral O_h
Instability coordinate	A''_2	E'	T_{1u}
Ground state	$^1A'_1[2p_z(N)]$	$^2A'_1[3d_{z^2}(Cu)]$	$^1A_{1g}[2p(O)]$
Excited state (cov)	$^1A''_2$ $2p_z(N) \rightarrow 1s\ (H)$	$^2E'$ $3s(Cl) \rightarrow 3d(Cu)$	$^1T_{1u}$ $2p(O) \rightarrow 3d(Ti)$
K^{cov}	-0.62 (mdyn/Å)	-2.85[a] ($10^{28}s^{-2}$)	
Excited state (pol)	$^1A''_2$ $2p(N) \rightarrow 3s(N)$	$^2E'$ $3d_{ry}(Cu) \rightarrow 3d_2(Cu)$	$^1T_{1u}$ $2p(O) \rightarrow 3s(O)$
K^{pol}	-0.06 (mdyn/Å)	-0.05[a] (10^{28} s^{-2})	
K^{cov}/K_{pol}	$1.03 \cdot 10$	$5.7 \cdot 10$	$1.1 \cdot 10$

[a] *In mass-weighted units*

treatment, mentioned above, in which the perturbation influence of the excited states explains the instability of the ground state and hence this influence is one of the possible reasons of instability, in the vibronic concept, formulated above, the vibronic mixing with appropriate excited states is the only possible source of instability. This means that *all the instabilities of high-symmetry configurations are of vibronic origin,* and hence, *if there is instability, there must be excited states that cause this instability.*

Thus we come to a formulation of the concept of vibronic interactions which reveals the mechanism of electronic control of configuration instability *via* vibronic coupling:

The reference configuration of any polyatomic system is unstable with respect to nuclear displacements Q if, and only if there are two or more electronic states that mix under these displacements, and the inequality (6) is obeyed.

The requirement of two or more mixing electronic states as a necessary condition of instability creates some new ways of thinking in chemistry. Indeed, it follows from this statement that stable configurations of molecules should be sought for among those with non-degenerate ground states and high energy excited states that are weakly admixing to the ground state by distorting nuclear displacements. On the other hand, any unstable high-symmetry configuration must be accompained by stable excited states. If we consider a reference configuration, its excited electronic states and their coupling to the ground state become most important in any possible changes of this configuration.

3. THE CRYSTAL FACTOR IN STEREOCHEMISTRY: SHORT-RANGE (CHEMICAL) VS. LONG-RANGE (COOPERATIVE) INTERACTIONS IN CONFIGURATION INSTABILITY

One of the major problems in transition metal stereochemistry is the role of the crystal factor, accentuated because many transition metal compounds are stable in the crystal state only. The question is whether the crystal lattice controls only the general stability of these compounds with respect to their component parts, or it determines also the local atomic configuration, or both. To address this aspect of the problem, let us consider the two main types of interatomic interactions in the crystal lattice:

(1) local, or short-range, i.e., interactions with nearest-neighbor atoms. These interactions are determined mostly by orbital overlaps and chemical bond formation, although there may be significant contributions from ionic (Coulomb) interactions and polarization;

(2) long-range interactions which are solely of pure Coulomb or dipole-dipole type.

The short-range forces control the local stereochemistry, whereas the long-range interactions produce temperature dependent cooperative effects resulting in lattice symmetry and/or structural phase transitions (at sufficiently low temperatures the crystal structure is determined by the potential energy only). Obviously, the long-range forces affect also the local symmetry, and it is not always clear to what extent the observed stereochemistry is due to local or long-range effects. In many cases, the widespread understanding is that the long-range interactions are the driving force for crystal lattice formation and structural phase transitions that

determine also the local symmetry. An interesting and illustrative example is provided by *displacive phase transitions* which are considered in more detail in the next section. In displacive phase transitions the local symmetry changes as a result of a relative shift of the crystal sublattices, and these changes are usually attributed to the long-range forces which compensate the local repulsion by distortion.

The vibronic theory allows for a better understanding of the underlying effects also in this field. As it is shown in the previous section, the instability of the reference high-symmetry configuration of the lattice is controlled by vibronic coupling with the corresponding excited states. According to Eqs. (2)-(9) the curvature of the adiabatic potential $K = K_0 + K_v$ contains two terms, K_0 and K_v, defined by Eqs. (4) and (9), respectively, K_0 being always positive, so a negative curvature and instability in the Q direction can be realized only when the negative vibronic contribution is sufficiently large, $-K_v > K_0$.

As stated above, K_0 is defined with the ground state wavefunction for the nuclei fixed at the reference configuration, Eq. (11). Since these wavefunctions do not change with the nuclear displacements Q, K_0 does not include the 'relaxation' of the electronic cloud which takes place by its following the displacing nuclei; this relaxation is included in K_v. On the other hand, it can be shown that *K_0 contains all the long-range forces, while K_v is essentially of local origin.* Indeed, in the expression (11) for K_0 the whole energy of the system E_0 after (12) is calculated with non-relaxed functions, while the contribution of the relaxation, as shown below, does not contain long-range interactions. In fact, K_0 contains all the Coulomb interactions in the crystal; this can be demonstrated by direct estimation of the matrix element (11) using the ground state wavefunction in the form of a determinant of MO LCAO functions (or any other one-electron approximation).

More illustrative is the fact that K_v contains local interactions only. This follows directly from the more detailed analysis of the origin of the vibronic contribution to the instability, given in the previous section. The terms of new covalency of the type (16) that originate from the vibronic mixing of atomic states from different atoms are essentially determined by the overlap of their wavefuncions $S(2p,3d)$. Indeed, aproximately, $\langle 2p|\partial H/\partial Q|3d\rangle \sim \partial H2p3d/\partial R \approx \partial S(2p,3d)/\partial R$, where H_{2p3d} is the corresponding resonance integral, and R is the interatomic distance.

Since S decreases exponentially with R, the covalency terms in K_v are negligible for all the next to near-neighbor interactions because of the near-zero overlap of their atomic wavefunctions. The polarization term is very small already for the near-neighbor interactions (Table 1) and, according to Eq. (14), it decreases with the interatomic distance as R^{-6}.

Thus the non-vibronic contribution to the curvature of the adiabatic potential K_0 contains all the long-range interactions, while the vibronic contribution K_v is essentially of local origin. But it has been proved that $K_0 > 0$, and only the negative contribution of K_v can make the curvature negative and the configuration of the system unstable. Hence *the long-range forces themselves cannot result in instability of the high-symmetry configuration of the lattice.* Since the vibronic contribution to the instability of the reference configuration is of primary importance, the main features of this instability, its direction and strength, are controlled by the local ground and excited states, their energies and wavefunctions.

However, this result does not mean that the long-range forces in the crystal play no significant role in the formation of the crystal lattice and the local stereochemistry. The condition of instability of the high-symmetry configuration with respect

to nuclear displacements (distortions) in the Q direction is that for this direction the inequality $-K_v > K_0$ (see Eq. (6), holds and is stronger than for other directions. Hence the directions for which K_0 is smaller (the lattice is softer) are most favorable for distortions. This means that for the same K_v values the direction of lattice distortion Q is determined by K_0, and there may be cases when for the actual distortion K_v is smaller than for other distortions due to a much lower K_0 value in this direction.

Another aspect of the issue is that, due to the long-range interactions, there may be directions of lattice distortions for which K_0 is lower because of lower Coulomb repulsions. For instance, for the off-center displacements of the Ti ion with respect to the oxygen environment and Ba atoms in $BaTiO_3$, mentioned above, K_0 is minimal when all the other Ti ions displace in the same way, i.e., the distortions are ordered (in the case in question — along one of the trigonal axes of the crystal). Therefore often the actual distortions at low temperatures coincide with the direction of the ordering. This creates an illusion that the distortions are produced by the ordering, i.e., they cannot exist without the long-range forces of the lattice; it is the main assumption of the theories of displacive phase transitions. As shown above, the long-range forces themselves may soften the lattice in certain directions, but they cannot produce instabilities without the local vibronic contribution. In the next section, a more detailed discussion of this topic is given using the problem of ferroelectricity in perovskite-type crystals as an example.

4. PEROVSKITE FERROELECTRICS. DO DISPLACIVE PHASE TRANSITIONS EXIST?

An interesting example that illustrate the role of local vs long-range forces in crystal stereochemistry and cast doubt on the very existence of displacive phase transitions is provided by perovskite ferroelectrics. The vibronic origin of local ion and lattice instability with respect to the displacements that produce dipole moments and spontaneous polarization in these systems, first suggested about three decades ago,[23] has recently been given new theoretical foundation and strong experimental evidence.[25]

Consider first the possible local off-center displacements of one Ti ion with respect to the near-neighbor oxygen octahedron and the remaining crystal lattice. In this case the titanium ion is regarded as a single impurity in the latice. Using some cluster model molecular orbital (MO) description of the electronic structure of the TiO_6^{8-} cluster and the Madelung potential of the remaining crystal lattice, we get the qualitative MO energy level scheme shown in Fig. 1; it is a typical MO LCAO scheme for octahedral transition metal d^0 systems.[8,10] The ground state of the system A_{1g} is formed by the occupied 12 oxygen $2p_\pi$ orbitals of t_{1u}, t_{2g}, t_{1g}, and t_{2u} symmetry (t_{1g} and t_{2u} are not shown in Fig. 1 as they are unessential), while the lowest unoccupied MO consists of the three $d_\pi(t_{2g})$ orbitals (d_{xy}, d_{xz}, d_{yz}) of Ti^{4+}. The t_{2g} orbitals of Ti and O form π bonds which are weak as compared with the main σ bonds.

The off-center displacements of titanium with respect to the oxygen octahedron and the remaining crystal are of the three-fold degenerate $T_{1u}(Q_x, Q_y, Q_z)$ type. Under these displacements, only the t_{1u} and the t_{2g} states become mixed. Neglecting the weak π bonding, the secular equation for the electronic energies as a function of these nuclear displacements $\varepsilon(Q\alpha)$, considering the linear terms of the vibronic

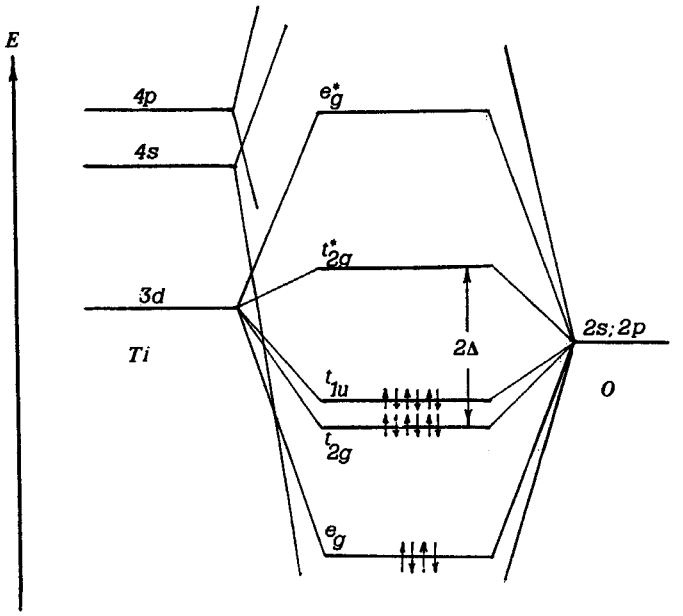

Figure 1 Qualitative MO LCAO energy level scheme for the TiO_6^{8-} cluster in the $BaTiO_3$ crystal.

coupling (5) as a perturbation, is of the 9th order (six $2p_\pi$ states of oxygen forming t_{1u} and t_{2g} combinations and the three t_{2g} states of Ti). Its roots can be determined directly.[12,23] The six electrons of the oxygens occupy the lowest three orbitals yielding the following adiabatic potential $W(Q\alpha)$ in the space of the T_{1u} displacement, which includes also the harmonic term of core interactions:

$$W(Q_x, Q_y, Q_z) = (1/2)K_0(Q_x^2 + Q_y^2 + Q_z^2) - 2\{[\Delta^2 + F^2(Q_x^2 + Q_y^2)]^{1/2} + [\Delta^2 + F^2(Q_x^2 + Q_z^2)]^{1/2} + [\Delta^2 + F^2(Q_y^2 + Q_z^2)]^{1/2}\} - 6\Delta \quad (17)$$

where 2Δ is the energy gap between the $2p_\pi(O)$ and $3d_\pi(Ti)$ states, $K_0 = M_0\omega_0^2$ is the bare force constant for the T_{1u} displacements determined by Eq. (4), and F is the vibronic coupling constant (3), mentioned above (Eq. (16):

$$F = \langle 2p_\pi^z(O)|(\partial H/\partial Q_x)_0|3d_{xz}(Ti)\rangle \quad (18)$$

The adiabatic potential surface (17) has very interesting features. If $K_0 > 4F^2/\Delta$, the surface has one minimum at $Q_x = Q_y = Q_z = 0$ with the titanium ion at the center of the octahedron. But if

$$4F^2/\Delta > K_0 \quad (19)$$

the point $Q\alpha = 0$ is a maximum (meaning instability), and there are eight minima at

$$|Q_x| = |Q_y| = |Q_z| = [(8F^2/K_0^2) - (\Delta^2/2F^2)]^{1/2} \quad (20)$$

at a depth

$$E^{(1)} = \delta = 3\Delta(Y + Y^{-1} - 2),\ Y = 4F^2/K_0\Delta \tag{21}$$

twelve saddle points at $|Q_p| = |Q_q| \neq 0$, $Q_r = 0$ (p, q, r = x, y, z) with a depth that lies between $E^{(1)}$ and $E^{(3)}$ (the latter is given below), and six saddle points at $|Q_p| = |Q_q| = 0$, $Q_r = [(16F^2/K_0^2) - (\Delta^2/F^{12})]^{1/2}$ with a depth $E^{(3)} = (2/3)E^{(1)}$.

Consider now the problem of vibronic instability of the lattice as a whole with respect to ferroelectric distortions. In the band structure formulation of the crystal as a whole[12,24,29] Q_x, Q_y, and Q_z are the optical phonon coordinates with the wave vector $q = 0$ which describe the mutual displacements of the titanium and oxygen sublattices. Approximately, the adiabatic potential surface is qualitatively (in the sense of the minima and saddle points relative positions) the same as in the local (titanium site) presentation, given above.[24,29] Omitting the calculations, we give here for illustration the condition of ferroelectric instability of the perovskite lattice of $BaTiO_3$:

$$M\omega_0^2 < 2F^2/\Delta_{eff} \tag{22}$$

$$\Delta_{eff} = \Delta[1 - h(h - S\Delta)/2\Delta^2]^{-1} \tag{23}$$

where ω_0 is the bare frequency of the ferroelectric displacements, (analog to the ω_0 value for the local T_{1u} displacements), M being the reduced mass of the elementary cell ($M\omega_0^2$ is the crystal analog to the local K_0), h is the resonance integral determining the band width of the valence band, and S is the $3d_\pi$ - $2p_\pi$ overlap integral.

Expression (22) is formally similar to Eq. (19), but the parameters are different from that in (19) (the factor 1/2 in the right hand side of (22) is approximately compensated by the fact that the M value in the left hand side is also smaller than the cluster value M_0). The most important difference between (19) and (22) is in the phonon frequency ω_0 which, due to the long-range forces, mentioned above, is obviously lower for the coherent (ordered) displacements of all the Ti atoms with respect to the oxygen sublattice, as compared with the displacement of one atom only. Together with the full qualitative similarity of the adiabatic potentials,[24] this conclusion means that, as far as only the internal energy is concerned and the entropy term is ignored, the ordered distortion of the crystal as a whole is preferable (however, see the discussion below).

Numerical estimates of vibronic instability[29] based on analytical band structure calculations show that for reasonable values of the lattice parameters and vibronic coupling constants the lattice may become unstable with respect to ferroelectric distortion and it has specific features of the adiabatic potential energy, described above. Recent numerical estimates of the vibronic coupling constants confirm this conclusion.[30] Band structure calculations for vibronic ferroelectrics using different techniques and also including dispersion of vibronic constants have been performed by different authors (see Ref[25,28,31,32] and references therein).

The special form of the adiabatic potential that emerges from the vibronic coupling allows for a direct interpretation of all the phases observed in $BaTiO_3$ and similar systems. *The main prediction of the vibronic theory* concerning these phases *is that only the low-temperature rhombohedral phase is fully ordered, the other two ferroelectric phases being, respectively, one-dimensional and two-dimensional disor-*

dered, and the paraphase is three-dimensionally disordered. Table 2 summarizes these results.

For the crystal as a whole, the problem of phase transitions in the lattice with the above adiabatic potential has been considered in a simple semiclassical model[28,33] in which the phase transition is considered as occurring at high temperatures when the amplitude of vibrations in the minima becomes sufficiently large and the system transfers from one minimum to another. At sufficiently low temperaures the crystal lattice has the configuration of the absolute minimum of the adiabatic potential which corresponds to the rhombohedral phase with all the Ti ions coherently displaced along the same trigonal direction.

By heating the system, first the lowest barrier between two near-neighbor minima *via* the orthorhombic saddle points is overcome resulting in an average orthorhombic polarization of the crystal (see below, Fig. 2). At higher temperatures the next barrier at the tetragonal saddle points is surmounted yielding an average (over four minima) tetragonal polarization. Finally, the last (highest in temperature) phase transition takes place when the motion of the crystal involves all the eight minima and the crystal, in average, is in the cubic paraphase (Table 2).

In this treatment, an estimation of the Curie temperatures T_c is also possible. They obviously depend on the parameters that determine the instability: the minima depth δ given in Eq. (21), and the positions of the corresponding saddle points. A simple modeling procedure in which the main features of the adiabatic potential are presented by two generalized parameters[33] allows us to make some estimations of T_c. Using the experimental T_c values for two phase transitions in $BaTiO_3$, $T_1 = 393$ K and $T_2 = 278$ K, we estimate the two parameters of the model and then, using their values, we get the third T_c value, $T_3 = 201$ K, while the experimental one is $T_3 = 183$. This result shows that the parameters involved and approximations made are not unreasonable.

Further qualitative estimates are possible based on the strong dependence of the vibronic parameters on the interatomic distances. Indeed, all the parameters in the condition of instability (19) or (22) and in the expression of the minima depth (21) are rather sensitive to the Ti–O distance R. In many cases their function of R is known qualitatively, by order of magnitudes. In particular, if we take into account (as in the previous section) that the integral of overlap between the oxygen $2p_\pi$ and titanium $3d_\pi$ AO is exponentially decreasing with R, $S(R) \approx \exp(-\alpha R)$, and the resonance integral h is proportional to S, $h \sim S$, and $\Delta_R \cong \Delta(1 + 2S^2)$ then we have approximately: $F \approx h' \approx S' = -\alpha S$, $\Delta' = -4\alpha\Delta S^2$, where primes denote derivatives with respect to R. On the other hand K_0 is also exponentially dependent on R but with a much stronger exponent power than in S (because it includes the overlap of all the bonding orbitals which is additive and much larger than for the above *p*

Table 2 Phases, phase transitions and disorder dimensionality in $BaTiO_3$ and $KNbO_3$ type crystals predicted by the vibronic theory.[23,25]

FEATURES	Rhombohedral	Orthorhombic	Tetragonal	Cubic
Direction of polarization	[111]	[011]	[001]	-
Dimensionality of disorder	**0**	1	2	3
Number of minima involved in disorder	-	two [111] and [1'11]	four	eight
Temperature of phase transition		Tc(I) <	Tc(II)<	Tc(III)

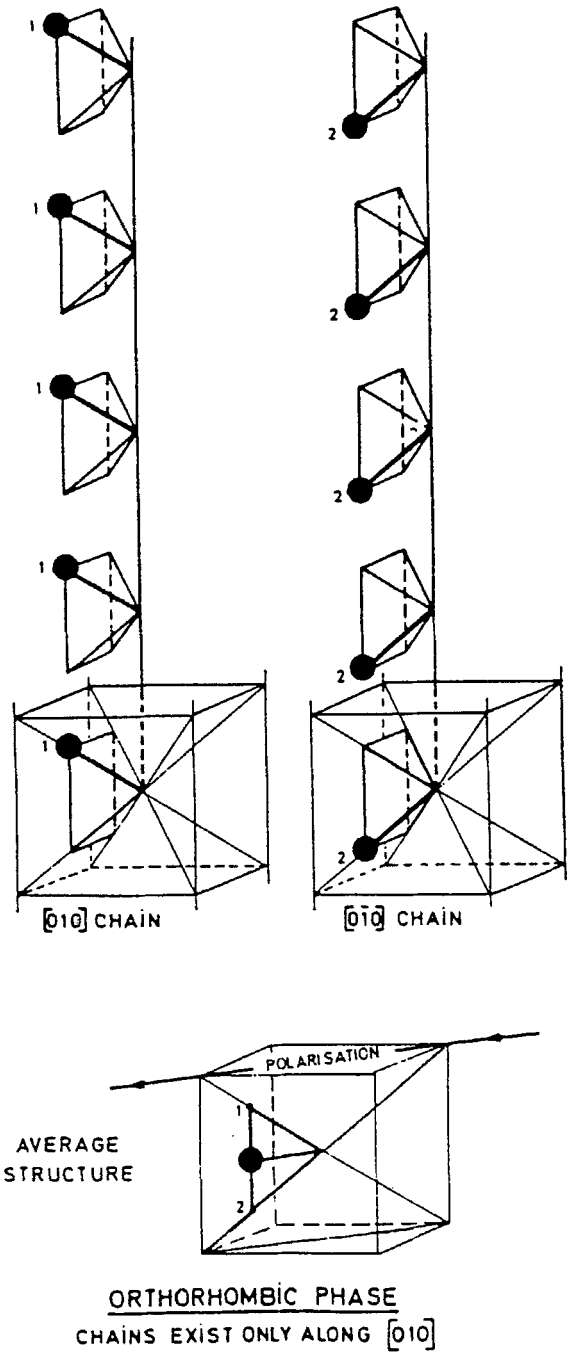

Figure 2 The Ti or Nb ion displacements in the [010] (left hand side) and [01'0] (right hand side) chains of the average orthorhombic perovskite structure (after ref. 36).

orbital): $K_0 \approx \exp(-\beta R)$, $\beta >> \alpha$. With these estimates and taking into account that T_c is determined by the minima depth δ, it can be shown that for sufficiently deep minima $T_c \approx \delta = 3\Delta(Y + Y^{-1} - 2)$, $Y = 4F^2/K_0\Delta$, $Y > 1$ (see Eqs. (19), (21)), and[25]

$$(T_c)'_R \approx 3\Delta(Y - Y^{-1})(\beta - 2\alpha) + 24\alpha\Delta S^2(1 - Y^{-1}) > 0 \qquad (24)$$

provided $\beta > 2\alpha$ which is quite reasonable.

Thus for ferroelectric perovskites the temperature of transition to the polarized (or more polarized) phases increases with the increase of the interatomic metal-oxygen distance. This explains directly the changes in ferroelectric properties along the series of titanates of Ca, Sr, and Ba in which the Ti-O distance R increases from left to right: $CaTiO_3$ is not ferroelectric, $SrTiO_3$ is a virtual ferroelectric (it becomes ferroelectric at very low temperatures under pressure or with appropriate impurities), while $BaTiO_3$ is ferroelectric at room temperature.[34]

A similar effect can be seen along the series of perovskites $BaMO_3$ with M = Ti, Zr, Hf, in which the active orbital of the metal that produces the vibronic contribution changes from 3d to 4d and to 5d, respectively, and the atomic radius of the metal increases. In effect this is similar to a decrease of the metal-oxygen distance which, following Eq. (24), decreases the Curie temperature and hence deteriorates the ferroelectric properties from left to right in this series. Quite similar phase transitions are observed in $KNbO_3$ and some other crystals with a perovskite structure.

Now let us approach one of the most important problems in this field, namely, the order-disorder vs displacive phase transitions in these crystals.

By definition, displacive phase transitions take place when the long-range forces in the lattice favor local distortions. In the case of $BaTiO_3$, the off-center displacements of the Ti ions with respect to the oxygens form a local dipole moment in each unit cell. These local dipole moments, if appropriately ordered in the lattice, create additional mutually attractive forces (as compared with the cubic structure) that lower the energy of the crystal. On the other hand, the local distortion produces additional Born repulsion (provided the vibronic coupling is not taken into account). If the attractive long-range forces are larger than the local repulsion forces that occur due to the distortion, then at sufficiently low temperatures the cubic configuration of the lattice loses its stability with respect to the above coherent displacements of the Ti ions[34] (phase transitions at higher temperatures take place due to the entropy factor).

As shown in the previous section, the long-range forces themselves cannot result in instability of the cubic lattice: only the contribution of the vibronic coupling, which is local in origin, makes the high-symmetry configuration unstable. It follows that *pure displacive phase transitions are most doubtful.* In $BaTiO_3$ the vibronic coupling yields a complicated adiabatic potential, discussed above, which shows that only the low-temperature rhombohedral phase is completely ordered, the others being partially disordered, in one direction in the orthorhombic phase and in two directions in the tetragonal phase, or completely disordered in the paraelectric phase (Table 2). This means that *the ferroelectric phase transitions in this crystal are of the order-disorder type.*

A further detailing of the nature of this order-disorder transition is possible if one takes into account the differences in the conditions of instability for a single Ti ion with respect to the remaining lattice (19) and for the lattice as a whole (22).[25] As

mentioned above, the latter is significantly softer than the former, because the K_0 value (or the $M\omega_0^2$ value for the crystal) decreases with increase of the number of ordered distortions. It means that distortion of the crystal as a whole in the ordered rhombohedral phase has the lowest potential energy U which increases with the disorder due to the increase of K_0. This is indeed the experimentally observed phase at sufficiently low temperatures. However, at higher temperatures the free energies, $E = U\text{-}TS$, where S is the entropy, should be compared instead of U.

Since disorder increases both the entropy S and the potential energy U, the condition of phase transition at $T = T_c$ (at which the free energies of the two phases should be equal) reveals the measure of disorder compatible with these conditions. It has been shown[25] that under certain conditions the disorder in the corresponding phases may not be complete; some ordered chain clusters may remain. For instance, at the phase transition from the completely ordered rhombohedral phase in $BaTiO_3$ to the orthorhombic phase, disordered in the [010] direction, a number of displacements of the Ti ion in the near-neighbor cells along this direction remain ordered, as shown in Fig. 2. The possible cluster structure of the disordered phases has been previously suggested.[35]

The number of ordered unit cells, N, in these clusters depends on the relative values of the entropy of disorder $r = T_c s/\delta$, where s is the entropy change per unit cell disorder, and δ is the depth of the adiabatic potential minimum created by the vibronic coupling in each cell (Eq. (21)), and on the relative value of the change in the bare force constant $p = (K_0\text{-}K_0^c)/K_0^c$, where K_0 and K_0^c are the bare force constants for the unit cell and the crystal as a whole, respectively, defined above. A rough estimation yields:[25]

$$N \approx N_0\text{-}(r/p) \tag{25}$$

Thus the most important prediction of the vibronic theory which makes it quite different from other theories is that the distortion forces are of local origin (hence the local distortions may be present in all the phases), and that the paraphase and the high-temperature ferroelectric phases occur as a result of a corresponding disordering of the local distortions. This prediction has been fully confirmed by a series of different kinds of experiments, some of which are listed in Table 3.

First we note the experiments of Comes, Lambert and Guinier[36] on diffuse scattering of X-rays in $BaTiO_3$. Qualitatively, these experiments confirm all the predictions of the theory[23,24] outlined in Table 2, including the partial disorder along one, two, and all the three directions in the orthorhombic, tetragonal, and para-phases, respectively. To comply with the observed entropy changes at the phase transitions, the authors[35,36] introduced the idea of ordered clusters in the disordered phases, discussed above.

The local and dynamic nature of the distortions in $BaTiO_3$ and $KNbO_3$ has been confirmed in a series of experiments on ESR with probing ions carried out by Muller and coworkers (for a review see ref. 37). For paramagnetic ions with a spin $S \geq 2$ (Fe^{3+}, Mn^{4+}, etc.) in cubic crystals there is an additional splitting in the ESR spectrum which is proportional to the local fourth-order crystal field potential. First, Fe^{3+} has been used as a probing ion to substitute for Ti in $BaTiO_3$ and, by comparison along a series of similar perovskites, it was shown that the fourth-order potential along the trigonal axis can be presented as $V(R) = -AR^2 + BR^4$ which has two minima at $R_m = \pm(A/2B)^{1/2}$ and an energy barrier between them $Vm =$

Table 3 Experimental evidence of local origin of distortions and order-disorder nature of phase transitions in 'displacive' ferroelectrics.

Authors, year	Method, system	Main result
Comes, Lambert, Guinier,[36] 1968	X-rays, diffuse scattering $BaTiO_3$	Qualitative confirmation of all the main predictions of the vibronic theory for $BaTiO_3$
Quittet et al.,[48] 1973	Raman spectra, $BaTiO_3$, $KNbO_3$	Polar distortions in the cubic paraphase
Burns, Dacol,[49] 1981	Optical refractive index, $BaTiO_3$	Nonvanishing component$<P^2>$ in the cubic phase
Gervais,[50] 1984	Infrared reflectivity, $BaTiO_3$	
Ehses et al.,[38] 1981	X-ray, $BaTiO_3$	Strong order-disorder component in the cubic phase
Itoh et al.,[39] 1985	X-ray, $BaTiO_3$	[111] displacement of Ti in the paraphase up to 180 K above T_c
Muller et.al.[37],1980	ESR with probing ion $BaTiO_3$, $KNbO_3$	[111] displacements in the rhombohedral phase and reorientations in the orthorhombic phase, $10^{-10}<t<10^{-9}$(sec)
Hanske-Petitpierre et al.,[40] 1991	XAFS, $KNb_xTa_{1-x}O_3$	[111] displacements in all the three phases for any x>0.08. Mean square displacements much smaller due to dynamics
Dougherty et al.,[41] 1992	Femtosecond resolution of light scattering, $BaTiO_3$, $KNbO_3$	No relaxational modes which might exclude the local distortion model
Sicron et al.,[44] 1994	XAFS, $PbTiO_3$	Ti and Pb ions are displaced in the paraphase up to 200 K above Tc

$(A/2)R_m^2$. The V_m value evaluated from the ESR data appeared to be larger by about 34% for $BaTiO_3$ as compared with non-ferroelectric perovskites. A similar strong anharmonicity is present in $KNbO_3$. These conclusions were confirmed by pressure and temperature dependence of the spectra.[37]

The results obtained by the Mn^{4+} probing ion are even more exciting. This ion substitutes Ti^{4+} in $BaTiO_3$, similar to Fe^{3+}, but distinct from the latter Mn^{4+} follows the displacements of Ti^{4+} (Fe^{3+} remains centered in the octahedron because of its lower positive charge and the presence of e_g electrons that are more strongly repulsed from the oxygens than the t_{2g} electrons of Mn^{4+}). The [111] displacement of the Mn^{4+} ion is seen from the axial crystalline splitting D = 0.65 cm^{-1} in the ESR spectrum of the rhombohedral phase. At the temperature of the phase transition to the orthorhombic phase the ESR signal disappears smeared out by transitions between the two near-neighbor minima (in $SrTiO_3$ the signal is visible in the whole range between 4 and 300 K). The lifetime τ in the minimum is estimated as (in sec.) $10^{-9} \leq \tau \leq 10^{-10}$. This relatively slow reorientation rate is attributed to the formation of the clusters, discussed above, and it explains why the Ti ion dynamics escape observation by neutron and Raman (or equivalent) scattering experiments, while in X-ray diffraction measurements it is seen in the paraphase as static distortion. The latter have been confirmed repeatedly by different authors[38,39] and show explicitly that the off-center displacements of the Ti ion is a local (not lattice) effect; in the displacive model there are no distortions in the cubic paraphase, neither local, nor cooperative.

New evidence of local origin of the distortions and their dynamics in the disordered phases is given by the X-ray absorption fine structure (XAFS) experi-

ments carried out recently[40] for $KTa_{0.91}Nb_{0.09}O_3$. This crystal undergoes qualitatively the same ferroelectric phase transitions as in $KNbO_3$ (and BaTiO), but at different temperatures with T_c = 85.6 K for the highest transition to the paraphase (the lower two being at 71 K and 80 K, respectively). The XAFS measurements which are a snapshot of the structure on a time equivalent of 10^{-16} sec, were carried out at T = 70, 78, 90, 130, 200, and 300 K, i.e. below and above the phase transition to the paraphase. At all these temperatures the Nb ion is displaced along the [111] direction of the oxygen octahedron by about 0.145 Å, with changes within 12% mainly at very high temperatures. Moreover, the mean-square displacements are much lower than the off-center ones indicating that the displacements are of dynamic nature.

The non-displacive nature of the phase transition is also confirmed by multiple measurements performed on the above crystal with different Nb concentrations: from a few percent through 100% of Nb the displacements of this ion remain the same within 10% of experimental uncertainties. This means that *there are no significant long range forces that influence the local distortions in this crystal.*

Support of the vironic model in application to $BaTiO_3$ and $KNbO_3$ has been obtained also by means of femtosecond resolution in light-scattering spectroscopy.[41] These results allowed one to eliminate some ambiguities in the previous light scattering experiments in which the above eight-minima (eight-site) model has been ruled out by assuming that in the light scattering experiments there are relaxational modes of the same symmetry as the soft modes, the former being masked by the latter. The assumed additional modes allowed the authors[42] to also eliminate the discrepancies between the values of the directly measured dielectric constant and that evaluated from spectroscopic data. The femtosecond spectra[41] confirm the absence of additional relaxational modes of the same symmetry as the soft mode (the relaxational mode due to ion reorientation has another symmetry), thus confirming the vibronic model, and giving an estimate of the dielectric constant of $KNbO_3$ and $BaTiO_3$ in accordance with other measurements (the discrepancies between the spectroscopic data[41] and direct measurements of the dielectric constant in $BaTiO_3$ were later eliminated by more exact capacitance measurements[43]).

Further experimental evidence of the local origin of ferroelectric distortions is provided by recent XAFS measurements on $PbTiO_3$ in a wide range of temperatures below and above the ferroelectric phase transition.[44] These results are of special interest for the theory since lead titanate is considered as a classical displacive ferroelectric; it displays a soft mode which is underdamped at all temperatures and a dielectric constant typical for displacive behavior. The main result of this work is that *the local distortions remain above the phase transition and do not disappear even at 200 K above* T_c. At this temperature the displacements of the Ti and Pb ions are still 70% and 60% of the corresponding low-temperature values, respectively. The cell distortions from the cubic structure change by only 15% from 12 K to 960 K.

This result strongly indicates that in this crystal, too, the distortion is of local origin as predicted by vibronic theory. The tetragonal distortions in this case are enhanced by the Pb ions. Indeed, the Pb^{2+} ion has two valence electrons $(6s)^2$ which in the cubic environment of the 12 oxygens form the so-called lone pair. The latter may be stereochemically very active due to the combined (A1g + T1u)-(eg + t_{2g} + t_{1u}) vibronic problem[10,12,45]. As shown below in section 7, the lone pair effect, under certain conditions, results in polar tetragonal distortions of the environment

(T_{1u} + Eg distortions), and this effect modifies the adiabatic potential: the eight equivalent minima become divided into two non-equivalent groups of four with lower energy in the direction of the tetragonal field produced by the Pb^{2+} ion (and there are six equivalent directions of such tetragonal distortions conforming to the symmetry of the crystal). Under the influence of this field the lower trigonal minima for the Ti ion are quenched becoming rather shallow. Still there may be some local states in them providing for the orthorhombic phase transition, presumably, observed at 183 K (with small changes of the structural parameters).

The strong tetragonal influence of the Pb ions explains also the much higher T_c value for the transition to the paraphase than in $BaTiO_3$ (Ba^{2+} has an electronic closed shell with high-in-energy excited states, and it is therefore inert), while for the next transition to the orthorhombic phase T_c is lower in the lead crystal. The small structural changes apparently observed at this phase transition indicate corresponding low energy barriers.

A series of numerical calculations of the adiabatic potential (total energy frozen-phonon calculations) of perovskite crystals in the approximation of the linearized-augmented-plane-wave method (wihtin the local density approximation) has been performed by Cohen and coworkers.[46,47] For $BaTiO_{13}$ the authors found absolute minima for the crystal in the direction of ordered trigonal displacements of the Ti ions along [111] and more shallow minima along the tetragonal directions. This agrees well with predictions of the vibronic theory. The calculations show also that the distortions are sensitive to the unit cell volume, the minima depths increasing with the latter. This result is also in agreement with that discussed above (Eqs. (21) and (24)). Another interesting conclusion from these computations is that the covalency of the Ti-O bond is essential in the ferroelectric instability which agrees with the conclusion of the vibronic theory that the vibronic instability is due mainly to new covalency formed by distortion.

5. LOCAL DISTORTIONS PRODUCED BY *d* ELECTRONS: $CuCl_5^{3-}$ *VS* $ZnCl_5^{3-}$ POLYHEDRONS

The general validity of the vibronic approach allows for its application to any stereochemical problems. In this section, an example is provided on how this approach can be used to solve the problem of the origin of significant differences in stereochemistry of transition metal compounds that differ only by the number of *d* electrons.

Consider two crystal structures, $[Co(NH_3)_6][CuCl_5]$ (I) and $[Co(NH_3)_6][ZnCl_5]$ (II), which differ by substitution of the Cu atom by Zn. The X-ray analysis and other investigaions[51-54] show that the pentacoordinated polyhedra $CuCl_5^{3-}$ (I) and $ZnCl_5^{3-}$ (II) in these crystals have essentially different shapes. Both are unstable in the D_{3h} trigonal/bipyramidal (TBP) configuration. The $CuCl_5^{3-}$ ion in the $[Co(NH_3)_6][CuCl_5]$ crystal is unstable with respect to E' type distortions describing the conversion toward a square-pyramidal (SP) configuration, TBP → SP (Fig. 3a), it has three equivalent (almost) SP configurations, and performs fast conversions between them (molecular *pseudo*-rotations). The $ZnCl_5^{3-}$ ion in a similar crystal $[Co(NH_3)_6][ZnCl_5]$ is also not TBP, but it forms a distorted tetrahedron plus one chlorine ion on (almost) the trigonal axis[51], and there are no *pseudo*-rotations. This

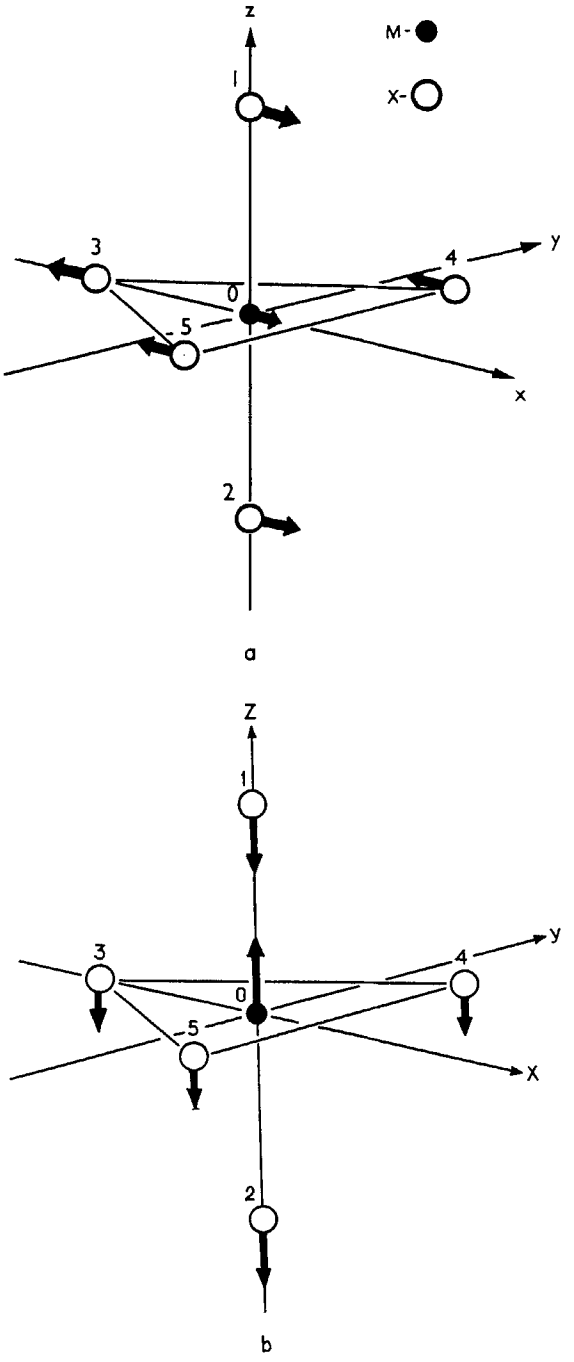

Figure 3 Ligand numeration and the main symmetrized distortions in pentacoordinated complexes MX_5^{n-}: (a) E′ type displacements realizing TBP → SP conversion (one of the three possible E' modes is shown); (b) A_2'' type displacement realizing the transformation $MX_5(TBP) \rightarrow MX_4(tetr.) + X$.

configuration can be regarded as produced by the A_2'' distortion of the TBP configuration, as shown in Fig. 3b.

The two different directions of distortions are evidently due to the difference in the electronic configuration of the central atom, d^9 (I) vs. d^{10} (II), and the question is whether this effect can be described by vibronic coupling, *i.e.*, by evaluating the ground and excited electronic states of the reference TBP configuration, estimating the values of the constants K_0, $F^{(0i)}$, and Δ, and the contribution of vibronic coupling to the instability of the ground state in different directions.

The problem has been considered recently.[27,55] The calculations have been carried out by the semiempirical MO LCAO iterative extended Hückel method with the excited states taken in the 'frozen orbital' approximation; they are formed by the corresponding one-electron excitations of the MO without recalculation of the appropriate self-consistent states. The numeration of the ligands is shown in Fig. 3. The six-atom system has 12 vibrational degrees of freedom, among which, in the D_{3h} group, three are of E′ and two of A_2'' symmetry. By means of special procedures[12] the calculation is reduced to the one-mode case.

As a result of the calculations of the electronic structure of $CuCl_5^{3-}$ in the TBP configuration, it was shown that the ground state is $^2A_1$ with the MO configuration $...(3e'')^4(5e')^4(5a_1')^1$ (Fig. 4). Satisfactory MO energy level ordering was obtained with the crystal field corrections (the Madelung potential) included. The single-occupied highest MO (HOMO) $5a_1'$ is an antibonding linear combination of the copper AO $3d_{z^2}$ and chlorine AO's $3p_\sigma$:

$$|5a_1'> = 0.60|3d_{z^2}> - 0.56(|3p_{\sigma 1}1> + |3p_{\sigma 2}>)$$
$$-0.23(|3p_{\sigma 3}> + |3p_{\sigma 4}> + |3p_{\sigma 5}) \quad (26)$$

The significant contribution of the metal $3d_{z^2}$ orbital to this MO agrees well with the ESR data. The MO 3e'' and 5e' are also antibonding linear combinations of the AO's $3d_{xz}$, $3d_{yz}$, $3d_{xy}$, of the copper atom with the AO's $3p_\pi$ and $3p_\sigma$ of the chlorine, respectively.

The electronic structure of $ZnCl_5^{3-}$ is qualitatively similar to $CuCl_5^{3-}$, but the MO energy level positions and occupation number, as well as the LCAO coefficients for these two systems differ significantly. In particular, the HOMO of II is also $5a_1'$, but as distinct from I it has other LCAO coefficients:

$$|5a_1'> = 0.18|3d_z2> - 0.60(|3p\sigma 1> + |3p_{\sigma 2}>)$$
$$-0.33\ (3p_{\sigma 3} + 3p_{\sigma 4} + 3p_{\sigma 5}) \quad (27)$$

and what is even more important, it is occupied by two electrons instead of one in I. This difference eliminates in II the excited states that originate in I from the one-electron transitions to this MO. Similar analysis can be made for the excited state contributions to the A_2'' displacements.[55]

By means of these occupied and unoccupied one-electron MO's, the excited states of E′ and A_2'' symmetry (for which the vibronic constants $F^{(A'E')}$ and $F^{(A'A'')}$ are non-zero) have been constructed, and the values K_0, Δ and F^2/Δ have been calculated. Some results are given in Tables 4 and 5.

Among the excited states of E′ type there are three states in I and two states in II whose vibronic admixture to the ground state gives the major negative contribution to the force constant. The first arises from the excitation of one electron from the fully occupied MO $|1e'> = 0.41(2|3s_3> - |3s_4>-|3s_5>)$ (formed

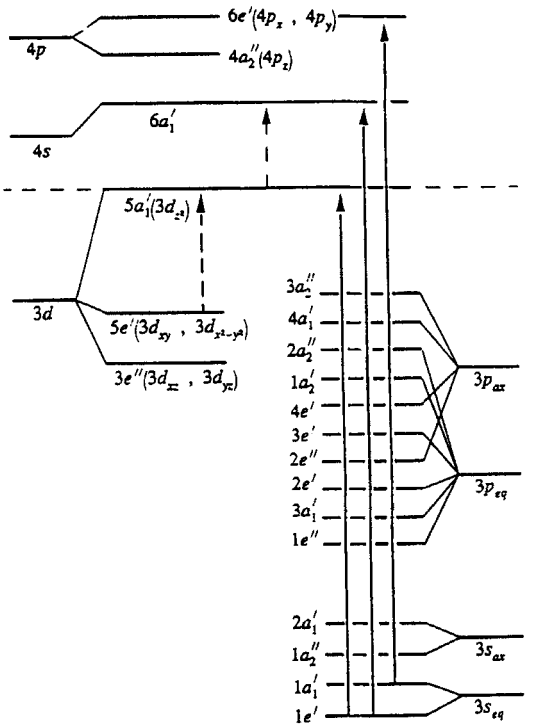

Figure 4 The MO LCAO energy level scheme for the complex $CuCl_5^{3-}$ in the TBP (D_{3h}) configuration with indication of the corresponding ligand AO (ax - axial, eq - equatorial). Solid arrows correspond to one-electron excitations generating the $^2E'$ excited electronic terms that give the maximum contribution to the instability *via* formation of new covalent binding. Dashed arrows show the excited states that originate from mainly intra-atomic excitation of the copper atom, their contribution to the instability *via* polarization of the latter being very small.

by the 3s AO's of the equatorial atoms) to the $5a_1'$ MO. This latter orbital is occupied by one electron in I and by two electrons in II, and therefore in the Zn complex there is no contribution of the $1e' \rightarrow 5a_1'$ excited state.

Although the energy gap to this E' term in I is large, the *pseudo* Jahn-Teller effect on the E' displacements is rather strong because of the relatively large vibronic constant $F^{(A'E')}$ for the mixing of the A_1' and E' states under consideration, which, in turn, is due to the strong alteration of the above MO by the distortion of the TBP configuration. Indeed, in the TBP configuration the overlap of the $5a_1'$ and $1e'$ orbitals is zero by symmetry restrictions (Fig. 5a), and hence these orbitals do not contribute to the metal-ligand bonding. The E' nuclear displacements lower the D_{3h} symmetry of the system to C_{2v}; as a result the e' MO splits into a_1 and b_2, while the $5a_1'$ orbital transforms to a_1. Now the overlap of $a_1(e')$ and $a_1(5a_1')$ is non-zero resulting in additional bonding of the $3d_{z^2}$ AO of the copper atom with the 3s AO's of the three equatorial ligands. This effect is not possible in II.

Table 4 Excited states of E′ and A_2'' symmetry produced by j→k one-electron excitations, energy gaps Δ = E(k)-E(j), orbital vibronic constants $F^{(oi)}$, and vibronic contributions $K_v^{(i)}$ and $K_0^{(d)}$ to the relative value of the force constant K_{rel} for the E′ and A_2'' displacements in $CuCl_5^{3-}$ (TBP configuration).

	j→K	Δ eV	$F^{(oi)}$ 10^{-4}dyn	$K_v^{(i)}$ mdyn/Å	$K_v = \Sigma_i K_v^{(i)}$ mdyn/Å	$K_0^{(d)}$ mdyn/Å	$K_{rel} = K_0^{(d)} + K_v$ mdyn/Å
E′	$1e'\rightarrow 5a_1'$	11.2	9.03	-0.91			
	$1e'\rightarrow 6a_1'$	25.0	12.24	-0.75			
	$1a_1'\rightarrow 6e'$	23.9	10.44	-0.57			
	$5e'\rightarrow 5a_1'$	2.8	0.58	-0.015			
	$5a_1'\rightarrow 6e'$	12.1	1.87	-0.036			
					-2.28	-0.35	-2.63
A_2''	$1a_2''\rightarrow 6a_1''$	24.4	11.68	-0.70			
	$3a_2''\rightarrow 6a_1'$	14.4	6.87	-0.41			
	$1a_1''\rightarrow 4a_2'$	26.5	7.97	-0.30			
	$1a_2''\rightarrow 5a_1'$	10.6	8.63	-0.88			
	$3a_2''\rightarrow 5a_1'$	0.8	1.72	-0.46			
					-2.75	-0.55	-2.20

The second active excited E′ term is formed by the promotion of one electron from the same occupied MO 1e′ to the virtual MO $6a_1'$ that has the predominant contribution of the 4s AO of the metal. In spite of large energy gaps (E($6a_1'$) - E(1e′) equal to 25.0 eV in I and 21.6 eV in II) the vibronic constants are also quite significant, and the corresponding negative contribution to the curvature, although somewhat smaller than for $1e' \rightarrow 5a_1'$, is of the same order of magnitude. This result is also due to the essential changes in the chemical bonding owing to the 1e′ and $6a_1'$ mixing by distortion. Similar to the previous case, the overlap of 1e′ with $6a_1'$ in the TBP configuration is zero by symmetry (Fig. 5b); the E′ distortion makes it non-zero resulting in additional chemical bonding between the metal 4s AO and the appropriate combination of 3s AO's of the equatorial ligands.

Finally, the third E′ type active excited state corresponds to the one-electron excitation from the occupied MO $|1a_1'> = 0.58(|3s_3> + |3s_4> + |3s_5>)$ to the virtual 6e′ MO that has the main contribution from the $4p_x$ ($4p_y$) AO of the metal atom. Here, again, the overlap between the $4p_x$ AO of the metal with the totally

Table 5 Excited states of E′ and A_2'' symmetry produced by j→k one-electron excitations, energy gaps Δ = E(k) - E(j), orbital vibronic constants $F^{(oi)}$, and vibronic contributions $K_v^{(i)}$ to the relative value of the force constant K_{rel} for E′ and A_2'' displacements in $ZnCl_5^{3-}$ (TBP configurtation).

	j→k	Δ eV	$F^{(oi)}$ 10^{-4}dyn	$K_v^{(i)}$ mdyn/Å	$K_v^{(i)} = \Sigma_i K_v^{(i)}$ mdyn/Å
E′	$1e'\rightarrow 6a_1'$	21.6	11.61	-0.78	
	$1a_1'\rightarrow 6e'$	24.4	10.07	-0.52	
				-1.30	
A_2''	$1a_2''\rightarrow 6a_1'$	20.7	10.84	-0.71	
	$3a_2''\rightarrow 6a_1'$	11.3	6.16	-0.42	
	$1a_1'\rightarrow 4a_2''$	26.9	8.92	-0.37	
					-1.51

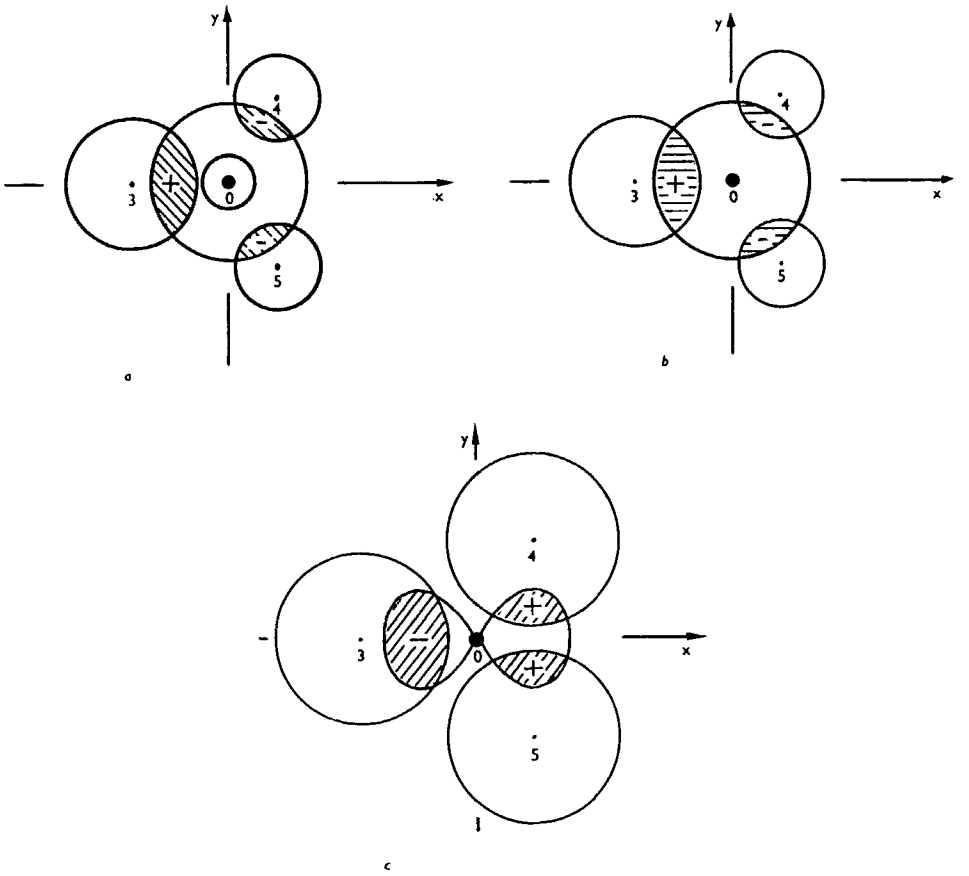

Figure 5 Schematic illustration to the covalency origin of the vibronic instability of the TBP configuration of $CuCl_5^{3-}$. Equatorial section of the trigonal bipyramid is shown. The overlap integral between the MO under consideration (hatched areas) is zero in the high-symmetry TBP configuration and becomes non-zero by E′ distortion transforming the equatorial equilateral triangle of the trigonal bipyramid into an isosceles triangle (the numbering of atoms is the same as in Fig. 3): (a) excited state $1e' \rightarrow 5a_1'$; the circles at the ligands present the 3s AO in the 1e' MO, their dimensions following the relative values of the LCAO coefficients, while the ring at the Cu^{2+} ion shows the equatorial cross-section of the d_{z^2} orbital forming the $5a_1'$ MO. (b) excited state $1e' \rightarrow 6a_1'$; the same as in (a) for the MO 1e', while the circle at the copper atom presents the MO $6a_1'$ that has predominant contribution from the 4s AO of the Cu atom. (c) excited state $1a_1' \rightarrow 6e'$; the same chlorine 3s AO form the $1a_1'$ MO (all the circles at the ligands are equal in dimension), while the lobs at the Cu atom present the MO 6e' that has the main contribution from the $4p_x$ AO of the metal.

symmetric combination of the 3s AO's of the equatorial ligands in the regular TBP configuration is zero (Fig. 5c), and the E′ displacements make this overlap non-zero with a consequent non-zero additional bonding with the equatorial ligands. All these processses for additional bond formation are accompanied by deterioration of other bonds. Obviously, the distortion takes place if the energy of the new bonds is larger that the increase of the appropriate strain energy.

The other E′ excited terms give negligible contributions to the configurational instability, as compared with that discussed above. The data on the vibronic

admixture of two other excited E′ terms are presented in Table 4 for system I. The first originates from one-electron excitation from the occupied 5e' MO with the main contribution of the Cu^{2+} $3d_{xy}$ and $3d_{x-y^2}$ AO's to the partly occupied $5a_1'$ MO (Fig. 4) where the LCAO coefficient of the metal $3d_{z^2}$ AO is also essential.

Because the main contribution to these MO's comes from the metal atom, the physical meaning of the vibronic mixing of the ground and excited terms is electronic polarization of the valence shell of the metal ion by ligand displacement (Section 2). Although the energy gap separating these electronic terms is much smaller than in the above cases, the value of the vibronic constant and therefore the corresponding contribution to the force constant is negligibly small (see the fourth row in Table 4 and Table 1).

To conclude whether the negative vibronic contribution K_v results in instability, the non-vibronic contribution K_0 must be calculated. Unfortunately, the semiempirical method used[27,55] does not allow one to do that: for calculation of K_0 the values of the wavefunction at the nuclei $\Psi(0)$ are required. Nevertheless the computational data, obtained above, enable us to estimate the relative instabilities induced by the vibronic coupling in different symmetrized directions of the same system, for which the K_0 value, in its part depending on $\Psi(0)$, can be assumed to be the same. In the cases discussed in this section we can compare the vibronic instabilities of the same system, I or II, with respect to the two possible distortions, E′ and A_2''. The contribution of the closed shell core electrons (and all the *ns* electrons) that make the $\Psi(0)$ quantity non-zero may be assumed the same for both distortions, whereas the contributions of the *d* hole to these two displacements are different.

Fortunately the *d* state contributions K_0^d to K_0 can be easily calculated.[55] The hole in the d^{10} configuration is d_{z^2}, and K_0^d is negative for E′ distortions and positive for A_2'' (the opposite signs are due to the field gradient created by the d_{z^2} hole which is positive in the *z* direction and negative in the *xy* plane).

The data in Tables 4 and 5 show explicitly that the $CuCl_5^{3-}$ complex is more unstable with respect to the E′ distortion that transforms the TBP configuration into SP (or near SP) (Fig. 3a), whereas in $ZnCl_5^{3-}$ the instability is stronger with respect to the A_2'' distortion that describes the transformation of the TBP configuration toward a distorted tetrahedron plus one ligand on the trigonal axis at a larger distance (Fig. 3b), in full qualitative agreement with the experimental data, mentioned above.

These examples show in detail how the electronic structure, ground and excited states, control the nuclear configuration making it, under certain conditions, unstable with respect to nuclear displacements of specific symmetry.

6. CRYSTAL ASPECTS: PLASTICITY, DISTORTION ISOMERS, TEMPERATURE DEPENDENT SOLID STATE CONFORMERS

In the previous section, the role of local interactions on the metal site geometry, as revealed by vibronic coupling, is emphasized. In this section, the discussion is continued by considering the new effects that emerge from the strong influence of the crystal environment on the local vibronically induced stereochemistry. We consider three effects: plasticity, distortion isomers, and temperature dependent solid-state conformers. The former two have been discussed in detail and reviewed

earlier;[8,56] they are given here again briefly in order to create a more complete picture of the subject. The latter effect has been studied recently by Simmons.[57]

6.1 Plasticity

Plasticity follows from the fact that, as a result of vibronic instability of the high-symmetry configuration, the system, if not decaying, has two or several or an infinite number of equivalent minima of the adiabatic potential with lower symmetry.[8,10] The consequent observable effects are usually termed as Jahn-Teller, *pseudo* Jahn-Teller, and Renner effects. If the molecular system is free, the multi-minimum adiabatic potential results first of all in special nuclear dynamics in which the molecule, roughly speaking, changes its configuration from one minimum to the other, equivalent.

Fig. 6 provides an illustrative example. For an octahedral system with a double degenerate electronic term Eg (Cu(II), Mn(III), Cr(II), *etc.*) the adiabatic potential in the space of the Jahn-Teller active e_g coordinates Q_ε and Q_θ (Fig. 7) in the linear

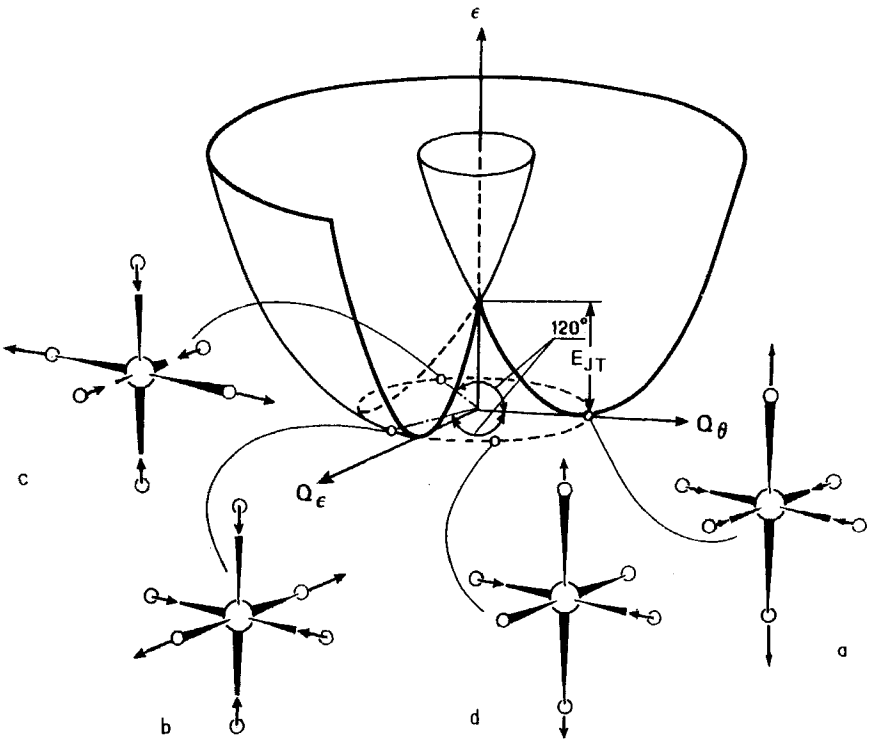

Figure 6 Jähn-Teller distortions of an octahedral system MX_6 at different points along the bottom of the trough of the 'Mexican hat' in the linear E-e problem. At the points ø – 0, $2\pi/3$, $4\pi/3$ the octahedron is tetragonally distorted along the three fourfold axes, respectively (a, b, c). In between these points the system has D_{2h} symmetry (d) and varies continuously from one tetragonal configuration to another within the circular trough $Q_\varepsilon^2 + Q_\theta^2 = \rho^2$ (for atomic displacements in the symmetrized Q_θ and Q_ε coordinates see Fig. 7).

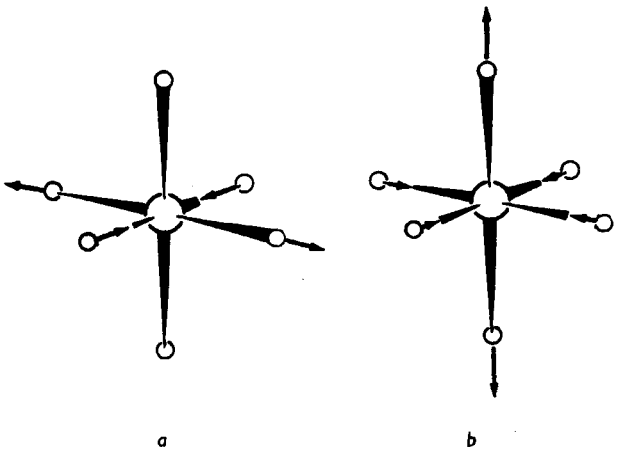

Figure 7 Symmetrized double degenerate Eg/type (tetragonal) displacements Q_θ (a) and Q_ε (b) of the ligands in an octahedral system MX_6.

approximation with respect ot the vibronic coupling terms has the shape of a 'Mexican hat' with an infinite number of equivalent minima that form a circular trough. Along the bottom of this trough, the system is distorted with minima point configurations $Q_\varepsilon^2 + Q_\theta^2 = \rho^2$, where ρ is the radius of the trough. Hence during the relatively slow nuclear motions along this potential near its minima (free 'rotations') its configuration changes as shown in Fig. 6.

If the quadratic terms of the vibronic coupling are taken into account, the Mexican hat becomes 'warped': three equivalent minima that correspond to tetragonal distorted octahedrons along the three axes, respectively (Fig. 6 a, b, c) occur along the trough. In this case hindered motion (or even pulse motions[8,10]) of nuclei takes place instead of free rotations in the linear case. In other cases of electronic degeneracies or in other reference configurations other types of nuclear dynamics are induced by the vibronic coupling.[8]

If the molecular system is not free, the external influence may quench these peculiar nuclear dynamics. In the case of the Mexican hat and free rotations of the distortions, mentioned above (Fig. 6), and external low-symmetry uniaxial perturbation in the tetragonal directions of the Jahn-Teller active coordinates (Q_ε and Q_θ, Fig. 7) creates an addditional minimum at a specific point in the trough; if this minimum is deep enough, the system may be 'trapped' and frozen in the configuration that corresponds to this minimum. The position of the additional minimum and hence the frozen configuration depends on the environment and changes with its symmetry. It follows, that among the many possible equivalent distortions of a coordination system predicted by the vibronic theory, only those in which the crystal state corresponds to the symmetry of the environment are realized, and in a measure allowed by this environment. Hence *the same coordination polyhedron may have significantly different shapes in different crystals.* This phenomenon looks as if the coordination polyhedron has a soft (plastic) coordination sphere which in the crystal state takes the form of the crystal environment; it is called *the plasticity effect*[8,56,58] (some authors prefer the term

'flexional behaviour'[59,60]). The first observation of this effect is due to Fackler and Pradilla-Sorzano.[60,61]

The best examples to illustrate the plasticity effect are octahedral coordination compounds with a two-fold degenerate E term (Cu(II), Mn(III), Cr(II), low-spin Co(II), *etc.*), mentioned above (Fig. 6). For these systems the adiabatic potential in the case of weak quadratic terms has the form of a Mexican hat which allows distortion of the coordination sphere along the symmetrized displacements that form the circular trough. If the quadratic vibronic terms are significant, only three directions of tetragonal distortion along the fourth-order axes remain equally probable.

For these systems the predictions of the theory are confirmed by a large amount of experimental data. The X-ray analysis shows that the six-coordinate polyhedron about these metals with E_g terms is not a regular octahedron even when all the

Table 6 Equatorial R_s and axial R_L interatomic distances Cu-O in Cu(II) compounds containing CuO_6 clusters (Ref. 8, 56).

Compound	R_S, Å	R_L, Å
$Cu(C_6H_4OHCOO)_2 \cdot 4H_2O$	1.88	3.00
$Cu(glycolate)_2$	1.92	2.54
$Cu(acac)_2$	1.92	3.08
$Na_2Cu(CO_3)_2$	1.93	2.77
$Na_2Cu(PO_3)_4$	1.94	2.52
$Cu(meso\text{-}tartrate) \cdot H_2O$	1.94	2.54
$Cu(OMPA)_2(ClO_4)_2$	1.94	2.55
$Cu(OH)_2$	1.94	2.63
$Cu_2P_4O_{12}$	1.95	2.38
$Cu(C_8H_5O_4)_2 \cdot 2H_2O$	1.95	2.68
CuO	1.95	2.78
$Ca(Cu,Zn)_4(OH)_6(SO_4)_2 \cdot 3H$	1.96	2.52
$PbCuSO_4(OH)_2$	1.96	2.53
$CuSO_4 \cdot 5H_2O$	1.97	2.41
$Cu(NaSO_4)_2 \cdot 2H_2O$	1.97	2.41
$Cu_6(Si_6O_{19})\text{-}6H_2O$	1.97	2.68
$Cu(C_2H_5OCH_2COO)_2 \cdot 2H_2O$	1.98	2.38
$CuWO_4$	1.98	2.40
$Tl_2[Cu(SO_3)_2]$	1.99	2.44
$Ba_2Cu(HCOO)_6 \cdot 4H_2O$	2.00	2.18
$Cu(HCOO)_2 \cdot 2H_2O$	2.01	2.37
$[C_{14}H_{19}N_2]Cu(hfacac)_3$	2.02	2.18
$CdCu_3(OH)_6(NO_3)_2\text{-}H_2O$	2.03	2.43
$K_2BaCu(NO_2)_6$	2.04	2.29
$Cu_4(NO_3)_2(OH)_6$	2.04	2.34
$Cu_4(NO_3)_2(OH)_6$	2.05	2.23
$Ca(Cu,Zn)_4(OH)_6(SO_4)_2 \cdot 3H_2O$	2.06	2.23
$Cu(OMPA)_3(ClO_4)_2$	2.07	2.07
$Cu(H_2O)_6SiF_6$	2.07	2.07
$Cu(IPCP)_3(ClO_4)_2$	2.07	2.11
$Cu(PCP)_3(ClO_4)_2$	2.11	2.04
$Ca(Cu,Zn)_4(OH)_6(SO_4)_2 \cdot 3H_2O$	2.11	2.11
$Cu(ClO_4)_2 \cdot 6H_2O$	2.13	2.28
$(NH_4)Cu(SO_4)_2 \cdot 6H_2O$	2.15	1.97

Abbreviations: acac = acetoacetate; OMPA = octamethylpyrophosphoramide; hfacac = hexafluoracetylacetonate; IPCP = tetraisopropymethylene-diphosphonate; PCP = octamethylmethylene-diphosphonic diamide.

ligands are identical, and in the majority of known cases the octahedron is tetragonally distorted. In Tables 6–9 some examples of crystallographically determined distances to the two axial (R_L) and four equatorial (R_L) ligands in a series of CuO_6 (Table 6), CuN_6 (Table 7) and other CuX_6 (Table 8) polyhedra, as well as in similar octahedral Mn(II) and Cr(II) systems (Table 9) are given (for a full list of such examples see ref.[8,56,62])

It follows from these tables that the six-atom polyhedra around the Cu(II), Mn(III), and Cr(II) centers in different crystals are mainly elongated octahedra, $R_L > R_S$, with two ligands on the long axis and four on the short axes. Although for some of the tabulated compounds the atoms from the second and next coordination spheres are different (and in the crystal the interatomic distances also depend on the packing of the molecules in the lattice), the large number of these compounds statistically confirms that the deformation of the coordination sphere around Cu(II), Mn(III) and Cr(II) is due to internal forces, *i.e.*, to the E term Jahn-Teller effect. This is also confirmed by the fact that in quite similar Zn compounds which have no ground state E terms there are no such distortions.

Table 7 Equatorial R_S and axial R_L interatomic Cu--N distances in Cu(II) compounds containing CuN_6 clusters (ref 8, 56).

Compound	R_S, Å	R_L, Å
β-Cu(phthalocyanine)$_2$	1.94	3.28
Cu(ethylenebidiguanide)$Cl_2 \cdot H_2O$	1.96	3.17
$Cu(C_4H_7N_5O)_2(ClO_4)_2$	1.97	3.14
$Cu(NH_3)_4(NO_2)_2$	1.99	2.65
$Cu(NH_3)_2(N_3)_2$	2.01	2.62
$Na_4Cu(NH_3)_4Cu(S_2O_3)_2 \cdot NH_3$	2.01	2.88
$Cu(phen)_3(ClO_4)_2$	2.05	2.33
$Cu(dien)_2Br_2 \cdot H_2O$	2.04	2.43
$Cu(N,N'\text{-}(CH_3)_2en)_2(NCS)_2$	2.06	2.52
$[Cuen_2]Hg(SCN)_4$	2.08	2.58
$Cu(1\text{-}pn)_3Br_2 \cdot 2H_2O$	2.09	2.31
$K_2PbCu(NO_2)_6$	2.11	2.11
$Cuen_3SO_4$	2.15	2.15
$Cu(dien)_2(NO_3)_2$	2.22	2.01
γ-$K_2PbCu(NO_2)_6$	2.23	2.05

Abbreviations: phen = o-phenanthroline; en = ethylenediamine; pn = 1,2-propanediamine; dien-diethylenetriamine; pn = -1,2-propandiamine

Table 8 Equatorial R_S and axial R_L distances Cu--X in Cu(II) compounds containing CuX_6 clusters, where X = F, Cl, Br (ref 8, 56).

Compounds	R_S, Å	R_L, Å
Ba_2CuF_6	1.85; 1.94	2.08
Na_2CuF_4	1.91	2.37
CuF_2	1.93	2.27
K_2CuF_4	1.92	2.22
$KCuF_3$	1.96; 1.89	2.25
$CuCl_2$	2.30	2.95
$(NH_4)_2CuCl_4$	2.30; 2.33	2.79
$CsCuCl_3$	2.28; 2.36	2.78
$CuBr_2$	2.40	3.18

Table 9 Equatorial R_S and axial R_L interatomic distances Me--X in some compounds containing MX_6 clusters, where M = Mn(III), Cr(II) and X = O, S, F, Cl, I (ref 8, 56).

Compounds	R_s, Å	R_L Å
$K_2MnF_5H_2O$	1.83	2.07
$(NH_4)_2MnF_5$	1.85	2.10
K_2NaMnF_6	1.86	2.06
MnF_3	1.79–1.91	2.09
Cs_2KMnF_6	1.92	2.07
Mn(trop)$_3$,I	1.94	2.13
Mn(trop)$_3$,II	1.94–1.99	2.09
CrF_2	1.99	2.43
Mn(acac)$_3$	2.00	1.95
$KCrF_3$	2.14	2.00
Mn(Et_2dtc)$_3$	2.38–2.43	2.55
$CrCl_2$	2.40	2.92
CrI_2	2.74	3.24

The fact that elongated octahedra are observed confirms the assumption of strong vibronic coupling and strong quadratic vibronic interaction in the E-e problem for the systems under consideration: one of the three adiabatic potential minima is stabilized by the crystal environment. For every case listed in Tables 6–9 the origin of the stabilizing low-symmetry perturbation of the environment can, in principle, be determined.

The octahedron of the first coordination sphere is regular for several compounds, which means that the distortions are not stabilized by the crystal environment or cooperative effects.[8,12] In other words, the phase transition to lower-symmetry structures due to cooperative effects has not taken place at the temperatures of the X-ray measurements and should be expected at lower temperatures. For some of these compounds (*e.g.*, $CuSiF_6 \cdot 6H_2O$, $KPbCu(NO_2)_6$, *etc.*) this point of view has been confirmed by ESR and other direct measurements.

Reported systems with tetragonally compressed octahedra, $(MH_4)_2Cu(SO_4)_2 \cdot 6H_2O \cdot 6H_2O$, $Cu(PCP)_3(ClO_4)_2$, $Cu(dien)_2(NO_3)_2$, $Cu(en)_3SO_4$, $Mn(acac)_3$, Ba_2CuF_6, *etc.*, need additional thorough investigation. In similar compounds (*e.g.*, the nitrate of bis(terpyridine)Cu(II), $Cu(en)_3Cl_2$, K_2CuF_4, $K_2PbCu(NO_2)_6$) a more careful study shows that in fact there are no tetragonally compressed octahedra but rather tetragonally elongated octahedra which, being antiferrodistortive ordered, give an average picture of diffraction similar to that for ferrodistortive ordered compressed octahedra. A similar conclusion about elongated octahedra instead of the compressed ones emerges from ESR investigation.[63]

In some cases the tetragonally compressed octahedral polyhedron around Cu(II) is presumably controlled by the structure of the lattice as a whole, and CuF_6 in a Ba_2ZnF_6 crystal may serve as an example.[64] Indeed, in this crystal the octahedral environment around Zn is compressed due to crystalline effects, and the substitution $Ba_2Zn_{1-x}Cu_xF_6$ with x up to 0.3 does not change the crystal structure and the compressed octahedral environment of Cu(II).

Another conclusion derived from the data in Tables 6–9 is about the diversity of Cu-O and Cu-N distances, which vary greatly from one system to another preserving some relationship between R_L and R_S. It is easily seen that R_L decreases

when R_S increases and vice versa. The expressions of the vibronic theory can be employed to obtain useful relations between the interatomic distances in question. If we pass from symmetrized to Cartesian coordinates and take into account the relations between them imposed by the circular trough and the quadratic coupling constant, we come to the following relationship:[8]

$$R_L(1 - 4\eta) + R_S(2 + 4\eta) = 3R_0^* \tag{28}$$

where η is a constant that depends on the quadratic coupling, and R_0^* is the averaged metal-ligand distance which is independent of the vibronic coupling.

Since the η value is small,[8] this relation is approximately linear in R_L and R_S for any series of compounds for which the averaged metal-ligand distances R_0^* do not change significantly (and the harmonic approximation employed above is valid). As seen from Fig. 8, the linear relationship (28) is approximately satisfied: all the points (R_L, R_S) fall within a narrow band along a straight line with deviations of about 10%. The points with extreme distortions to the left and right of this band clearly lie outside the assumed harmonic approximation (large distortions acquire cubic and higher order displacements). This result confirms the vibronic nature of the observed distortions.

If a_L and a_S are the values at which the line (28) intersects the R_L and R_S axes, respectively, then

$$\eta = (2 - C)/4(1 + C) \tag{29}$$

where $C = a_L/a_S$ is the tangent of the angle of line slope. For the lines in Fig. 8 $C = 1.4$ and $\eta = 0.063$. This allows one to estimate the value of the radius of the circular trough $\rho = (2\sqrt{3})(R_L - R_S)$ and hence the vibronic coupling constants.

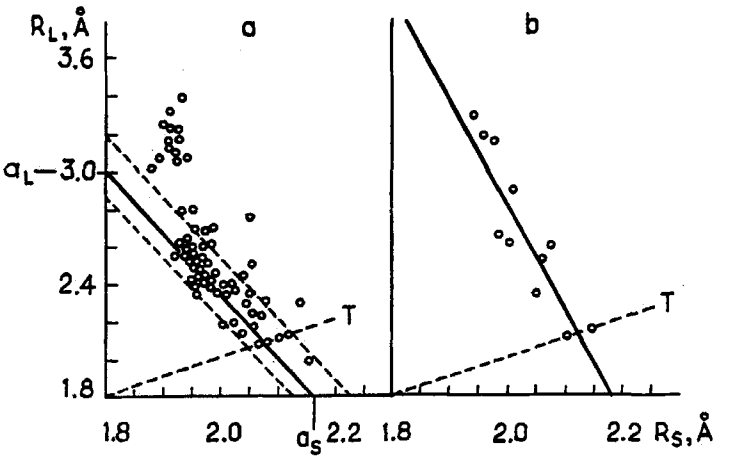

Figure 8 Axial (R_L) *vs.* equatorial (R_S) metal-ligand distances in octahedral clusters of divalent copper: (a) CuO_6, (b) CuN_6. With the exception of very large R_L, for which the harmonic approximation is invalid, the points (R_L, R_S) lie approximately within a narrow band near a straight line. T denotes the line $R_L = R_S$ (after ref 8).

6.2 Distortion Isomers.

It is possible for a crystal to stabilize not one, but two or several configurations of the coordination sphere which are close in energy differing by the distortion magnitude and direction. Such configurations of the same compound may exhibit themselves as different crystal isomers. An interesting example of this kind is the so-called distortion isomers of Cu(II) first synthesized and studied by Gazo et.al.[56,62] They possess the same total composition and the same Cu(II) ligand environment, but differ in the interatomic metal-ligand distances (in the distorted coordination sphere). These distortion isomers also differ in their properties, such as color, appearance, crystal form, chemical behavior, solubility, spectroscopic properties, *etc.* The isomers pass from one to another under the influence of pressure, heating or long-term storage. In some cases, besides the two principal isomers (usually called α and β), a series of intermediate species have also been synthesized.

One of the simplest compounds having distortion isomers is $Cu(NH_3)_2X_2$, where X = Cl, Br. A possible Jahn-Teller origin was suggested when the isomers were discovered, but understanding of their local *pseudo* Jahn-Teller and cooperative crystal nature was reached later.[56,58] The vibronic approach gives a natural explanation of the origin of distortion isomers as due to the vibronic properties of the Cu(II) center accompanied by the stabilizing infuence of and cooperative effects in the crystal.

Consider the crystal $Cu(NH_3)_2X_2$ as an example. It comprises mutually parallel chains, each being arranged as illustrated in Fig. 9a, where all the X atoms occupy equivalent bridge positions. There is a strong interaction between the Cu(II) centers

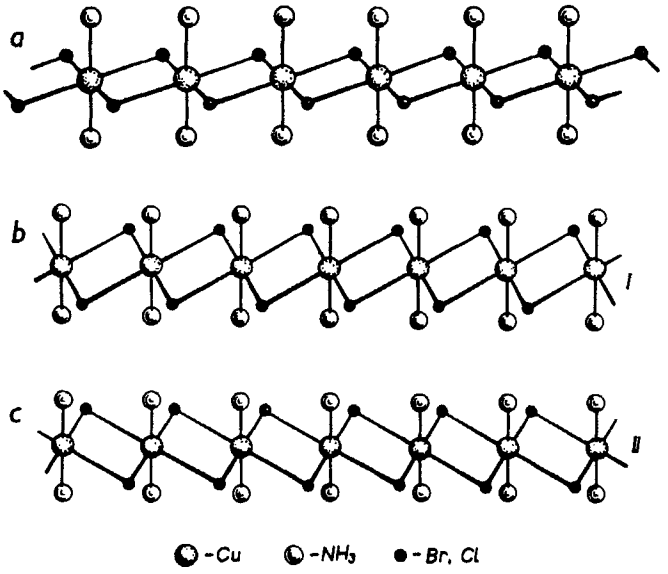

Figure 9 Chain structure of the crystal $Cu(NH_3)_2X_2$ in the cubic undistorted unstable β isomer (a), and in two equivalent configurations of the α isomer, I and II (b and c), resulting from the in-chain cooperative *pseudo* Jähn-Teller effect (after ref. 8, 56).

through bridging atoms inside the chain, while the bonding between the chains *via* van der Waals interactions and/or hydrogen bonds is weak. Each copper atom is surrounded by four X atoms in the plane of the square and by two NH_3 groups in the *trans* positions 1 and 4. The degeneracy of the Cu(II) ground state in the octahedron is removed as a consequence of the difference between X and NH_3, and the ^2E_g term splits into $^2A_{1g}$ and $^2B_{1g}$ with the splitting of 2Δ.

If we assume that the X atoms in the plane form a regular square, the polyhedron $Cu(NH_3)_2X_4$ is a tetragonally distorted octahedron belonging to D_{4h} symmetry. The *pseudo* Jahn-Teller effect on the A_{1g} and B_{1g} terms of such a complex at each center distorts the bipyramid environment along the B_{1g} coordinate Q_ε (Fig. 7) in such a way that the square of its base with four atoms X at the apices transforms to a rhombus with the major diagonal along Q_x corresponding to the minimum I in Fig. 9, or along Q_y (minimum II).

Due to the strong interaction between the distortions of neighboring centers in the chain through the common ligands X, a ferrodistortive ordering along the chain takes place, and this ordering remains unchanged up to high temperatures. As a result, it can be assumed that at room temperature each of the chains has two stable configurations, I and II (Fig. 9b and c) corresponding to two minima for each center (I and II in Fig. 10). We conclude that there is a possibility that two equivalent chain structures of $Cu(NH_3)_2X_2$ originate from the *pseudo* Jahn-Teller effect at each bipyramidal center $Cu(NH_3)_2X_4$ with ferrodistortive ordering of the distortions due to cooperative effects.

One more important crystal factor remains to be considered: the interaction between chains. The analysis of the structure of the crystal composed by parallel chains indicates that intermolecular interaction between the chains is optimum when the chains are not distorted and the entire crystal is cubic. In this cubic state the intermolecular distances (between the strongest interacting atoms of different chains) are minimal, and they increase with intra-chain distortions towards configuration I or II. The inter-chain interaction as a function of the interatomic

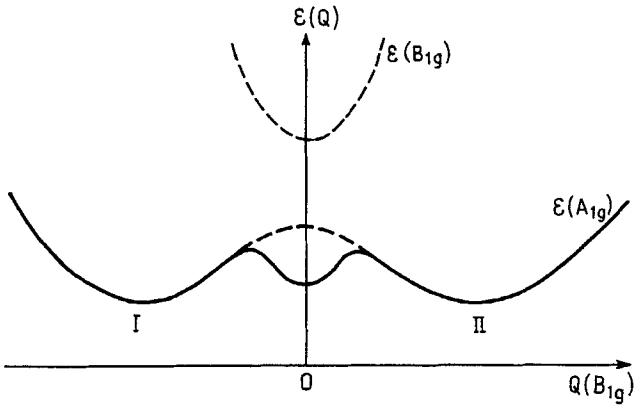

Figure 10 Energy curve for the $Cu(NH_3)_2X_2$ crystal as a function of the cooperative ferrodistortive intra-chain distortion which is of B_{1g} symmetry on each center. I and II correspond to the *pseudo* Jähn-Teller minima, while the additional minimum at $Q(B_{1g}) = 0$ corresponds to the best-fit inter-chain interactions of undistorted chains (dashed lines).

distance can, in principle, be estimated semiempirically (say, by means of the atom-atom potential approach). We assume that the inter-chain interaction in the crystal has a minimum at Q = 0 (Fig. 10), where Q is the coordinate of the cooperative intra-chain distortion corresponding to the B_{1g} distortion at each center. The total energy of the crystal schematically shown in Fig. 10, under the above assumptions has three minima: besides two minima I and II for the stable distorted configurations of the chains, there is a third minimum for the undistorted crystal.

It is assumed above that all chains are in the same type of minimum, either I, or II, and the intra-chain distortions are ordered along the crystal. If different chains are in different types of minima (and the entire crystal is not ordered) the total energy may have additional minima which, however are expected to be more shallow than the minima I and II, but deeper than the minimum at Q = 0 (on the assumption that the intra-chain *pseudo* Jahn-Teller stabilization energy is larger than that of the inter-chain interactions).

It can be shown that the above description explains qualitatively the origin of all the main features of the distortion isomers in $Cu(NH_3)_2X_2$. The α isomer corresponds to the deepest minimum of the adiabatic potential (I or II) with the structures illustrated in Figs. 9b, and c. The unstable β isomer with the cubic structure corresponds to the more shallow minimum at Q = 0, and the intermediate preparations with non-cubic structures correspond to the above-mentioned additional relative minima for the uncorrelated chain distortions. The interpretation agrees well with the experimental features of the isomers, including their behavior under stress and temperature, the dependence on conditions of their preparation, spectral properties, transitions from one isomer to another, *etc.*[56,62]

It is noteworthy that good crystals (single crystals) can be obtained only for the β isomer,[62] *i.e.,* when (as follows from the theory), the intermolecular (inter-chain) interactions, favoring crystal formation, are maximum. On the contray, the α isomer and intermediate preparations cannot be obtained in the form of good crystals (but only as powders), in agreement with the assumption of poor inter-chain interaction in these situations. The fact that the β (and only the β) isomer contains NH_4X compounds as impurities may also be important. The crystal NH_4X crystallizes in the cubic structure isomorphic to the β isomer of $Cu(NH_3)_2X_2$, and these two systems easily form mixed crystals. Apparently, the cubic structure of the β isomer is also stabilized by the large amount of NH_4X impurity molecules, which alternately occupy the places of Cu(II) centers in the chains, strongly reducing the intra-chain effect. It has been shown[65] that without the NH_4X admixture the β isomer converts to the α isomer much more rapidly than with such admixtures, but the pure β isomer can still be prepared and preserved under pressure.

The *pseudo* Jahn-Teller origin of the intra-chain distortions has also been confirmed by approximate calculations of the *pseudo* Jahn-Teller distortions of the $Cu(NH_3)_2X_4$ polyhedron.[66]

Other examples of distortion isomers have been discussed,[8,56] in particular, the one based on dioxymes of trivalent cobalt and rhodium of the type $[Co(DH)_2APh_3Hal]$, where DH is dimethylglyoxymate $[CH_3(HON)C = C(NO)CH_3]$; A = P, As, Sb; $Ph_3 = (C_6H_6)_3$, Hal = Cl, BrI.

6.3 Temperature Dependent Solid State Conformers

This kind of flexible vibronic configuration in crystals was first shown by Simmons to occur when there are two or more rapidly converting vibronically distorted configurations which are slightly inequivalent due to the crystal influence, and the observed averaged configuration is thus temperature dependent.[57]

Consider the system $[Cu(bpy)_2(ONO)]NO_3$ with the copper polyhedron *cis*-CuN_4O_2. In the high-symmetry configuration of $[Cu(bpy)_3]^{2+}$ (bpy = bipyridine) the system has D_3 symmetry with the two-fold degenerate ^2E ground state. The substitution of one of the bpy groups by ONO reduces the symmetry to C_2 and splits the ^2E term into ^2A and ^2B. Similar to the distortion isomers discussed above, there is possibility of a *pseudo* Jahn-Teller effect and consequent instability of the ground state ^2A with respect to Q_B displacements ($A \times B = B$), provided the vibronic coupling constant $F = \langle A|\partial H/\partial Q_B|B\rangle$ is sufficiently large and the inequality (2) or (6) holds. The Q_B displacements emerge from Q_ε (Fig. 7) and have the same geometry.

Assuming that the inequality (2) is satisfied, we get, for the adiabatic potential curve as a function of the coordinate Q_B, the picture shown in Fig. 11 together with an indication of the modes of distortion of the CuN_4O_2 polyhedron in the minima.

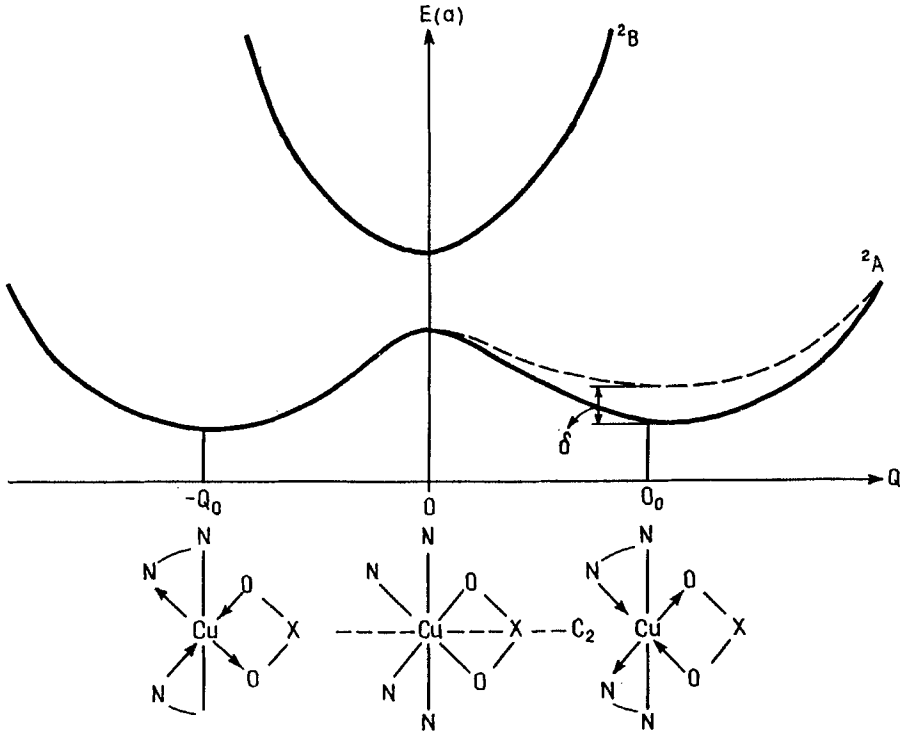

Figure 11 Two minima of the adiabatic potential in the $[Cu(bpy)_2(ONO)]NO_3$ crystal with a strong *pseudo* Jähn-Teller effect on each center and slightly different minima depths due to the crystal environment, the influence of the next coordination sphere.

The value of the distortion coordinate Q_B (the coordinate $Q_\varepsilon = (1/2)(X_2 - X_5 - Y_3 + Y_6)$ in octahedral systems, Fig. 7) in our notation for the *cis*-CuN_4O_2 polyhedron is (the index B is omitted):

$$Q = (1/2)[\Delta R(Cu-N_1) + \Delta R(Cu-O_1) - \Delta R(CuN_2) - \Delta R(Cu-O_2)] \quad (30)$$

where N_1, N_2, O_1 and O_2 are the two nitrogen and two oxygen atoms in the plane containing the C_2 axis (Fig. 11), and ΔR denotes the elongation of the bond with respect to that in the high-symmetry configuration. For linear distortions $\Delta R(Cu-N_1) - \Delta R(Cu-N_2) = R(N_1) - R(N_2)$ and $\Delta R(Cu-O_1) - \Delta R(Cu-O_{12} = R(O_1) - R(O_2))$, where R(X) is the bond length Cu–X and

$$Q = (1/2)[R(N_1) - R(N_2 + R(O_1) - R(O_2)] \quad (31)$$

In the unstable high-symmetry configuration $Q = 0$, while in the two minima $Q = \pm Q_0 \neq 0$. If the energy barrier between the minima (*i.e.*, the *pseudo* Jahn-Teller stabilization energy) is not very large, the system converts rapidly between the minima, and in some methods of observation (say, in X-ray diffraction methods) the averaged undistorted configuration will be observed (if the minima are shallow and there are no local states in them, the averaged configuration will be observed by all methods[10]).

The situation changes when, due to the crystal environment, the two minima become slightly nonequivalent, as shown in Fig. 11 by the dashed line, but the energy difference δ between the minima is smaller than the barrier height (otherwise the second minimum disappears). In this case there is no complete averaging over the two configurations because the two minima are not equally populated. Denoting the relative populations of the two configurations by n_1 and n_2, gives according to Boltzman populations

$$n_2 = n_1 \exp(-\delta/kT) \quad (32)$$

with the normalization

$$n_1 + n_2 = 1 \quad (33)$$

Then the observed thermally averaged distortion is:

$$Q_{av} = (n_1 - n_2)Q_0 \quad (34)$$

or

$$Q_{av} = Q_0[1 - \exp(-\delta/kT)]/[1 + \exp(-\delta/kT)] \quad (35)$$

Thus the observable averaged distortion O_{av} is temperature dependent, its absolute value being determined by both Q_0 and δ.

These distorted configurations of the same compound which change gradually with temperature can be called *temperature dependent solid-state conformers.* At high temperature when $kT >> \delta$, in the first order with respect to δ/kT, $\exp(-\delta/kT) \approx 1 - (\delta/kT)$ and

$$Q_{av} = Q_0\delta/2kT \quad (36)$$

In the opposite limit case when $kT << \delta$, $\exp(-\delta/kT) \approx 0$, and $Q_{av} \approx Q_0$.

The observed distortions in $[Cu(bpy)_2(ONO)]NO_3$ and similar systems[57] follow these rules rather well. The atomic structure of this compound has been determined in four temperature regions: 20, 100, 165, 296 K. Table 10 shows the corresponding

Table 10 Bond lengths R(X) = R(M--X) (in Å) and distortion coordinate Q_{av} in MN_4O_2 polyhedra of $[M(bpy)_2(ONO)]NO_3$ with M = Cu at different temperatures, and for M = Zn.

	M = Cu			M = Zn	
	20K	100K	165K	296K	295K
$R(N_1)$	2.142(2)	2.110(2)	2.098(2)	2.085(2)	2.085(2)
$R(N_2)$	2.028(2)	2.060(2)	2.071(2)	2.074(4)	2.082(3)
$R(O_1)$	2.536(2)	2.414(2)	2.351(3)	2.320(5)	2.204(3)
$R(O_2)$	2.051(2)	2.155(2)	2.204(3)	2.230(5)	2.223(3)
Q_{av}	0.299	0.155	0.087	0.050	0.008

interatomic distances and the value Q_{av} calculated after (31) for different temperature, as well as the same data for $[Zn(bpy)_2(ONO)]NO_3$ at 295 K, for comparison. In the last compound there is no *pseudo* Jahn-Teller effect of the kind present in $[Cu(bpy)_2(ONO)]NO_3$ and hence no temperature dependent conformers are expected.

The data in Table 10 are typical for temperature dependent solid-state conformers; the temperature dependence of Q_{av} closely follows Eq. (35). In particular, if we assume that at T = 20K $Q_0 \approx Q_{av} = 0.3$, while at T = 296 K Eq. (36) holds, we obtain directly: $\delta = (Q_{av}/Q_0)2kT \approx 69\ cm^{-1}$. The author[57] performed a more exact estimation: $\delta = 74\ cm^{-1}$. Note that in Zn(II) Q_{av}, as expected, is small to zero, and the absence of conformers in the Zn(II) compound is also seen from the temperature factor in X-ray experiments.[57]

The solid-state conformers under consideration differ from each other in interatomic distances, and in this sense they are similar to distortion isomers, discussed above. However the latter coexist at the same temperature, whereas different conformers are observed at different temperatures, and the larger the temperature difference, the larger the structural differences of the conformers. Also important is that structural changes in conformers take place gradually with changes in temperature in contrast to structural phase transitions which take place abruptly at a certain temperature.

7. LOCAL DISTORTIONS PRODUCED BY $(ns)^2$ LONE PAIRS

Lone pairs, *i.e.*, pairs of electrons with opposite spins which do not participate in the bonding, play an important role in stereochemistry. In the semiclassical considerations mentioned in the introduction to this paper, the lone pairs are considered as repulsive units alongside the bond pairs, and as such, they occupy a coordination position distorting the otherwise symmetrical coordination polyhedron.[3] However in some systems the polyhedron is not distorted, in spite of the presence of a lone pair, and in these cases the latter is called an inactive or *'inert lone pair'*.[6]

Very often the lone pair originates from the central atom $(ns)^2$ configuration, with n = 4, 5, 6, *i.e.* the post transition elements In (I), Tl(I), Pb(II), Sb(III), Te(IV), Xe(VI), *etc.* In $SbBr_6^{3-}$ and $TeCl_6^{2-}$, for example, the $(ns)^2$ lone pair is stereochemically inert (the octahedron is not distorted), whereas in XeF_6, $InCl_6^{5-}$, *etc.*, the octahedron is distorted. The $(ns)^2$ pair itself is spherical-symmetrical and does not cause distortions. Hence using the VESPR model in order to explain the origin of

distortion, one has to assume that there is a strong hybridization of the ns states with the np ones resulting in a directed lone pair.[67,68]

On the other hand, hybridization is in fact not the cause of the distortions but rather its consequence. In the more general MO LCAO scheme the distortion occur if, in the high-symmetry configuration the two electrons occupy a strongly antibonding MO which under the distortion transforms to a lone pair.[15] All these considerations are qualitatively true, but do not assist in a more general solution of the problem.

The vibronic approach provides understanding of the origin of the lone pair effect and a criterion for when it occurs and what kind of distortions it may produce. Consider the general MO LCAO scheme (Fig. 12) for an undistorted octahedral system MX_6 which in the representation of local M-X σ bonds has a $(ns)^2$ electron pair above the six bonding pairs (in fact each M-X bond may have more than one bonding electron pair, as in the case of multiple bonds). In this scheme the two ns electrons occupy the antibonding MO a_{1g} (π MO and ligand non-bonding MO's are not indicated). The ground state of the system, A_{1g}, is non-degenerate, but relatively close-in-energy are the excited T_{1u} states formed by one-electron excitations $a_{1g} \rightarrow t_{1u}$.

In the vibronic approach the stability or instability of the regular octahedral configuration under consideration is determined by Eq. (2) which gives the parameter relationship for which the system is unstable, and the direction of instability. The *pseudo* Jahn-Teller mixing of the $^1A_{1g}$ ground state with the excited $^1T_{1u}$ by T_{1u} type nuclear displacements results in the instability of the ground state with respect to T_{1u} distortions, provided the condition (2) is satisfied. This distortion is somewhat similar to the dipolar instability produced by the same A_{1g}-T_{1u} mixing in the TiO_6^{8-} octahedron (Section 3), but the change from *d*

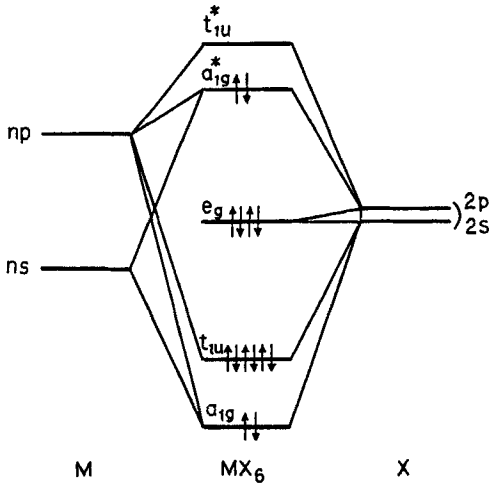

Figure 12 The MO LCAO energy level scheme for an MX_6 system with a $(ns)^2$ configuration above the closed shells of M and X. Six ligand σ (or hybridized *sp*) AO and the central atom ns and np AO form the bonding a_{1g} and t_{1u} MO and the non-bonding e_g MO occupied by 12 electrons, while the antibonding MO a_{1g}^* is occupied by the two $(ns)^2$ electrons (π MO and ligand non-bonding MO are not indicated).

electrons in Ti to *sp* electrons in the MX_6 systems under study in this Section introduces significant alterations. It can be shown that in the linear approximation with respect to the vibronic coupling terms in the Hamiltonian the *s-p* (A_{1g}-T_{1u}) vibronic mixing (the ($A_{1g} + T_{1u}$)-t_{1u} problem[12]) results in a trough of minima in the space of T_{1u} distortions (it means that all the distortions corresponding to any combination of the three T_{1u} coordinates has the same energy), and only the second order terms make the eight trigonal directions preferable.

However, as shown recently[69], this problem may be complicated by the fact that the excited T_{1u} term is degenerate and hence it is subject to the Jahn-Teller T_{1u}-($e_g + t_{2g}$) effect.[8,12] Thus the vibronic problem as a whole is a combined *pseudo* Jahn-Teller and Jahn-Teller problem ($A_{1g} + T_u$)-($t_{1u} + e_g + t_{2g}$) meaning that there may be distortions of three types: T_{1u}, E_g and T_{2g}. The solutions obtained in the linear approximation with respect to the vibronic coupling terms in (1) show that several possibilities arise dependent on the vibronic coupling constants and the energy gap 4Δ between the ground A_{1g} and excited T_{1u} states. We denote by F, F_E, and F_T the coupling constants to the T_{1u}, E, and T_{2g} displacements, by K_0, K_0^E, K_0^T the respective bare force constants (see Section 2, Eq. (4)), and the energies of the two mixing terms by $E(^1A_{1g}) = -3\Delta$, $E(^1T_{1u}) = \Delta$, and introduce the following constants:

$$f = F^2/(K_0\Delta)$$
$$e = F_E^2/(K_0^E\Delta) \qquad (37)$$
$$t = F_T^2/(3K_0^T\Delta)$$

These constants have the physical meaning of corresponding Jahn-Teller stabilization energies in units of Δ, taken from an appropriate read off.

In these denotations the expected distortions of the regular octahedron in MX_6 systems under consideration can be evaluated analytically[69] (in the paper[69] totally symmetric distortion are also included). The results are illustrated in Fig. 13, which include two coinciding schemes, one for e *vs.* f, and the other for t *vs.* f. The meaning of these schemes is as follows. The area limited by the axes e and f (or t and f) is divided into three domains, E_1, E_2, and E_3, that have different kinds of adiabatic potential minima. In the first domain (dotted area) where $f < 1$, $e < 1$, and $t < 1$, the Jahn-Teller and *pseudo* Jahn-Teller stabilization energies are smaller than the corresponding threshold given by Eq. (2), and hence there are neither Jahn-Teller, nor *pseudo* Jahn-Teller distortions. This is the case for on inert lone pair.

In the area where $f > 1$ the *pseudo* Jahn-Teller T_{1u} (dipolar) distortion becomes operative, but the admixing of the excited T_{1u} term involves the Jahn-Teller T_{2g} and E_g distortions, too. According to the calculations,[69] the relative energies of the minima in the three domains in Fig. 13 are (in Δ units):

$$E_1 = -6$$
$$E_2 = -6 - [2(-1)^2/(f - t) \qquad (38)$$
$$E_3 = 2 - 8t$$

and the same relations with e instead of t for the e-f plane. Therefore the trigonal dipolar (*pseudo* Jahn-Teller) distortions T_{1u} with admixture of either E_g or T_{2g} distortions are preferable when $E_2 < E_3$ which yields, in addition to $f > 1$,

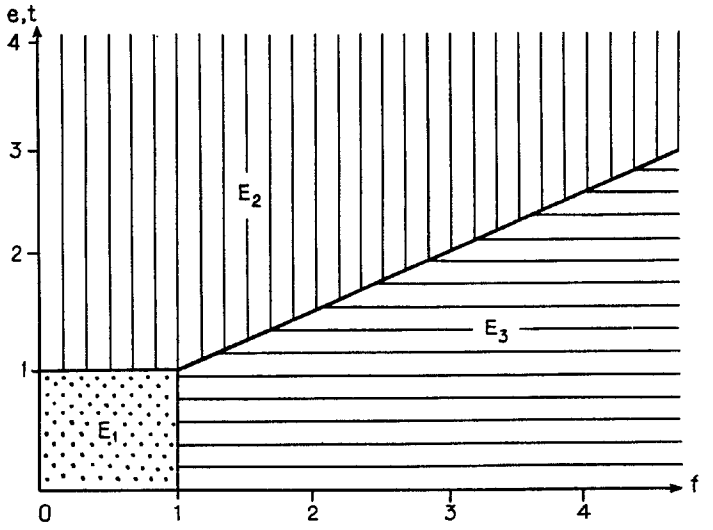

Figure 13 Three domains of existence of different Jähn-Teller and *pseudo* Jähn-Teller distortions in MX_6 systems with $(ns)^2$ lone pairs in each of the two e-f and t-f planes: E_1 - no distortions (inert lone pairs); E_2 - combined dipolar T_{1u} and either tetragonal E_g (in the e-f plane), or trigonal T_{2g} (in the t-f plane distortions; E_3 - pure Jähn-Teller either tetragonal (in the e-f plane) or trigonal (in the t-f plane) distortions.

$$f + 1 > 2t \tag{39}$$

and

$$f + 1 > 2e \tag{40}$$

respectively. If the opposite inequalities hold, *i.e.*, if

$$2e > f + 1 \tag{41}$$

or

$$2t > f + 1 \tag{42}$$

then the tetragonal D_{4h} or trigonal D_{3h} Jahn-Teller minima of the T_{1u} excited state are lower in energy (than the assumed ground state), and they are active in stereochemistry. The preference between tetragonal or trigonal minima is the same as in the usual Jahn-Teller $T_{1u} - (e + t_{2g})$ problem,[8] namely, the trigonal distortions are preferable if $t > e$, and the tetragonal ones occur for the opposite inequality, $e > t$.

All these distorted configurations of MX_6 systems with $(ns)^2$ lone pair configurations are found in different systems (see ref.[1-7,13,70,71] and references therein). Moreover, the combined distortions, described above, explain the origin of complicated (helicoidal) crystal structures.[72] In particular, in the InCl crystal ($InCl_6^{5-}$ units) both types of distortions in the E_2 area of Fig. 13, trigonal T_{2g} plus dipolar T_{1u}, and tetragonal E_g plus dipolar T_{1u}, are observed in two phases of the crystal, yellow and red, respectively. Another example with polar tetragonal (T_{1u} + E_g) distortions is $PbTiO_3$, mentioned above in Section 4.

A similar, in principle, treatment is possible for many other types of systems. In particular, in multi-center transition metal clusters the change of geometry from, say, regular tetrahedral in 60-electron tetraclusters to butterfly geometry in similar 62-electron clusters was subject to discussion from the point of view of a vibronic problem on two electronic terms $T_1 + T_2$ mixing *via* $Eg + T_{2g}$ distortions.[73,74] Many observed cluster geometries can be explained in this way.

8. VIBRONIC MUTUAL INFLUENCE OF LIGANDS

The mutual influence of ligands on stereochemistry can be considered as an effect of vibronic interactions. Indeed, the substitution of one ligand in the coordination system by another can be regarded as a change in the electronic structure which produces changes in the nuclear configuration *via* vibronic coupling. In Section 2 the main equations of vibronic instability are given, which show that any changes in the electronic structure may produce corresponding changes in the nuclear configuration; the vibronic coupling theory also shows how the ligand geometry changes by coordination.[8] A similar idea is used in this section to consider the mutual influence of ligands or, more precisely, the change in mutual influence by changing ligands.[75–77]

Consider a homoligand coordination system of the type MX_n with a non-degenerate electronic ground state. Its Hamiltonian can be presented as

$$H = H_{el} + W \tag{43}$$

where H_{el} is the electronic part of the Hamiltonian for fixed nuclei and W contains the vibronic coupling terms of (1). In the stable configuration $Q\alpha = 0$, $\alpha = 1, 2, ..., N$, the adiabatic potential $\varepsilon(Q\alpha)$ has a minimum with respect to all symmetrized coordinates $Q\alpha$, and in the harmonic approximation $\varepsilon(Q\alpha)$ gas the usual quadratic form with $K\alpha$ given by Eq. (4).

Upon substitution of the ligand X by Y, the change of the Hamiltonian (43) can be presented by adding the so-called substitution Hamiltonian H_s equal to the difference between the Hamiltonians of the $MX_{n-1}Y$ and MX_n systems:

$$H = H_{el} + W + H_s \tag{44}$$

Assuming that H_s can be considered as a perturbation, implies that changes in energy states provided by H_S are small. Then to obtain the adiabatic potential of the system with the Hamiltonian (44), one must consider two perturbations, H_S and W, instead of W only in the MX_n system. With the two perturbations the adiabatic potential $\varepsilon'(Q\alpha)$ is:[75]

$$\varepsilon'(Q\alpha) = \varepsilon(Q\alpha) + h_{00} - \Sigma_j h_{0j}^2/\Delta_{j0} - 2\Sigma_{\alpha,j}(h_{0j}F\alpha^{0j}/\Delta_{j0})Q\alpha \tag{45}$$

where we denoted

$$h_{0j} = \langle 0|H_s|j\rangle \tag{9.35}$$

while

$$F\alpha^{0j} = \langle 0|(\partial H/\partial Q\alpha)_0|j\rangle \tag{47}$$

are the vibronic constants (*cf.* (3)), Δij being the energy gaps (5). From Eq. (45) one can see that in addition to the constant terms h_{00} and $-\Sigma h_{0j}^2/\Delta_{j0}$ which do not

depend on Q and just produce a shift of the energy levels, there is a term linear in $Q\alpha$. Added to the quadratic terms in $\varepsilon(Q\alpha)$, this linear term displaces the minimum position in the $Q\alpha$ directions with the sign of this displacement determined by the sign of the product $h_{0j}F^{0j}$. The new equivalent positions are:

$$Q\alpha^0 = 2\Sigma_j h_{0j} F\alpha^{0j}/\Delta_{j0} K\alpha o \tag{48}$$

where $K\alpha o$ is given by (4).

Thus the vibronic treatment of mutual influence of ligands implies that by substitution of one of the ligands changes the electronic structure which is hence no longer consistent with the previous geometry, and other ligands relax to new equilibrium positions (new minima of the adiabatic potential). To find the new positions matrix elements of the vibronic coupling (the vibronic constants F^{0j}) and the substitution operator h_{0j} should be analyzed. This can be done by considering concrete systems using a model description.

Consider, for example, the MO LCAO model for octahedral σ-bonded complexes MX_6 of the following three basic types:

(i) M is a transition element, and there are 12 electrons in the valence σ MO's.
(ii) M is a post-transition element in a low oxidation state, and there are 14 electrons in the σ MO's (*i.e.*, there is an electron lone pair).
(iii) M is a post-transition element in a higher oxidation state.

The typical MO energy level schemes for these systems are illustrated in Fig. 14. By populating the one-electron MO with the number of valence electrons available, we easily find the highest occupied MO (HOMO) and the lowest unoccupied MO (LUMO). For the group (i) the HOMO is t_{1u}, while the LUMO is e_g^*, for (ii) the HOMO and LUMO are a_{1g}^* and t_{1u}^*, respectively, and so on (Table 11).

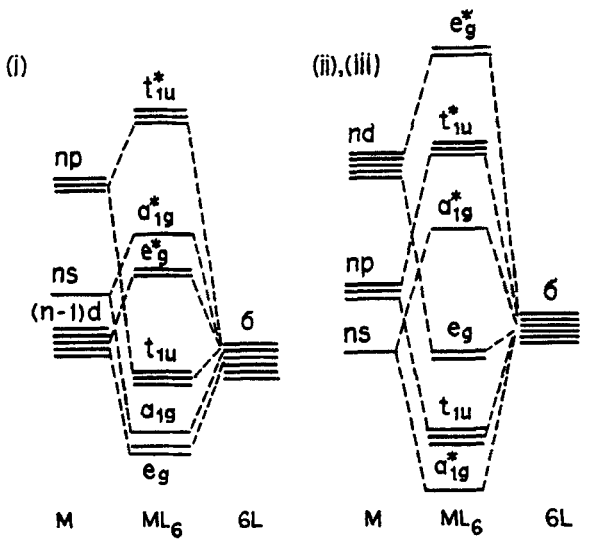

Figure 14 Typical σ MO energy level schemes for octahedral MX_6 complexes of transition (i) and post-transition (ii, iii) elements. The HOMO are: (i) t_{1u}, (ii) a_{1g}^*, (iii) e_g (for the denotations (i), (ii), (iii) see the text).

Table 11 The parameters characterizing the distortions in σ bonded complexes of transition and post-transition elements produced by the substitutions $MX_6 \rightarrow MX_5Y$ in octahedral and $MX_4 \rightarrow MX_3Y$ in square-planar complexes (ref. 75). CA - central atom.

Type of complex	HOMO	LUMO	Distortion mode for which $F\alpha \neq 0$	AO of CA for which $h \neq 0$	Distortion coordinate $Q\alpha$
Octahedral:					
(i)	t_{1u}	eg^*	T_{1u}, T_{2u}	p_z, d_{z^2}	$Q_z'' = (Z_1 + Z_4)/\sqrt{2}$
(ii)	a_{1g}^*	t_{1u}^*	T_{1u}	s; p_z	$Q_z'' = (Z_1 + Z_4)/\sqrt{2}$
(iii)	e_g	a_{1g}^*	Eg	d_{z^2}; s	$Q_\theta = (2Z_1 - 2Z_4 - X_2 + X_5 - Y_3 + Y_6)/\sqrt{12}$
Square-planar:					
(i)	e_u	b_{1g}^*	E_u	p_x; $d_{x^2-y^2}$	$Q_x = (X_2 + X_4)/\sqrt{2}$
(ii)	a_{1g}^*	e_u^*	E_u	s; p_x	$Q_x = (X_2 + X_4)/\sqrt{2}$

The next step of simplification is to restrict the treatment to HOMO and LUMO only, a restriction which is often used in quantum chemistry. With the HOMO-LUMO constraint there is only one off-diagonal matrix element (46) $h_{01} = h$, only one vibronic constant $F_{01} = F$, one energy gap $\Delta_{10} = \Delta$, and (48) simplifies significantly:

$$Q\alpha^0 = 2hF_\alpha/\Delta K_\alpha \tag{49}$$

Thus only one type of symmetrized coordinates is non-zero, and this is determined by the selection rules. Indeed, the vibronic constant after (47) is non-zero if the product of the irreducible representations Γ of the ground $|0>$ and excited $|1>$ states contains the irreducible representation of the derivative of the Hamiltonian with respect to $Q\alpha$. The representation of this derivative coincides with that of $Q\alpha$. Hence for non-zero $F\alpha$, it is required that $\Gamma_0 \times \Gamma_1$ contains Γ_α.

For instance, for complexes of the case (i), $|0>$ and $|1>$ are the HOMO and LUMO t_{1u} and e_g^*, respectively, and since $T_{1u} \times Eg = T_{1u} + T_{2u}$, only $Q(T_{1u})$ and/or $Q(T_{2u})$ distortions can, in principle, occur as a result of the above substitution $MX_6 \rightarrow MX_5Y$. On the other hand, the non-zero distortion after (49) also requires that $h = <0|H_s|1>$ should be non-zero, which means that the HOMO and LUMO should contain the atomic orbital of the substituted atom. To obey this condition, if Y is on the z axis, the t_{1u} and e_g^* MO should contain the p_z and d_{z^2} orbitals of the central atom, respectively. With these orbitals, F is non-zero for $Q(T_{1u})$ only, namely for its Q_z'' component:[75] $Q_z'' = (Z_1 + Z_4)/\sqrt{2}$. This distortion displaces the two ligands in the *trans* position 1 and 4 along the z axis (both of them in the same direction) with respect to the plane of the central atom and the other four ligands. In the same manner the distortion coordinates $Q\alpha$ active in the mutual influence of ligands have been obtained for other types of coordination systems shown in Table 11.

Thus within the limits of the HOMO-LUMO approximation the coordinates of mutual influence for a ligand can be revealed directly without detailed calculations. As seen from the Table 11, the distortions induced by ligand substitution are, indeed, directed, and for the most part these directions are along the *trans*-coordinate (*trans*-influence); in the case (iii) in octahedral σ-bonded complexes of non-transition elements in high oxidation states, the active coordinate is Q_θ (Fig. 7)

which yields both *trans* and *cis* displacements with opposite signs, the *cis*-influence being weaker than *trans* by half.

But the picture as a whole remains incomplete, even qualitatively, without knowledge of the sign of $Q\alpha$. Following (49), the sign of $Q\alpha$ is determined by the sign of the product $hF\alpha$, so we should analyze the signs of h and $F\alpha$ after (46) and (47). For this purpose the values of the LCAO coefficients for the HOMO and LUMO may be useful. A detailed analysis shows[75,76] that this issue can be solved by estimating the value of the matrix element $h \approx \langle 0|H_s|1\rangle$ for the substitution $X \rightarrow Y$ as proportional to the difference between their Coulomb integrals: $h \approx \Delta\alpha = \alpha(Y) - \alpha(X)$. The latter characterize their corresponding ionization potentials or σ-donor properties. Omitting the calculations, we bring here some of the main results.

Let us assume that by substitution $X \rightarrow Y$ the σ-donor properties increase, *i.e.*, $\Delta\alpha = \alpha(Y) - \alpha(X) > 0$. Then it can be shown[75] that for octahedral σ-bonded coordination compounds of group (i) (transition metals with 12 electrons on the six σ MO) $h < 0$, $F > 0$, and hence for these systems $Q_z'' < 0$. This distortion is equivalent to *trans*-elongation because in $Q_z'' = (Z_1 + Z_4)/\sqrt{2}$, $Z_1 = Z_4$, and hence $Z_4 < 0$. For $\Delta\alpha < 0$ the *trans*-elongation changes to *trans*-shortening. Note that in this approximation the *cis* ligands are not involved in the mutual influence. In complexes of the type (ii), $F < 0$ and $h > 0$, and hence $Q_z'' < 0$. Thus in octahedral σ-bonded complexes of non-transition elements with 14 electrons in the σ MO's (one lone pair) the distortion by ligand substitution is similar to that expected for group (i): *trans*-elongation for increasing σ-donor properties, $\Delta\alpha > 0$, and *trans*-shortening when the opposite inequality $\Delta\alpha < 0$ holds. Many examples in the literature confirm these conclusions.[78–80]

In compounds of the third kind (iii), post-transition element complexes in high oxidation states, the situation is more complicated and further differentiations must be introduced.[75] The MX_6 compounds of this group must be divided into two classes according to the position of their σ energy levels of X in Fig. 14 with respect to that of M. The compounds of post-transition elements M from the left hand side of the Periodic Table, for which the energy levels of the ns valence AO are located about the same level or even above the σ AO of typical ligands, fall into the first class. For the right hand side elements the ns AO lies below the σ AO of the ligands, and compounds of these elements form the second class.

For the first class of compounds from group (iii) $F > 0$ and for $\Delta\alpha > 0$ $h < 0$. Hence for these compounds the sign of the Q_θ distortion (Table 11) is negative: $Q_\theta < 0$. From the form of Q_θ displacements given in Fig. 7, one can see that $Q_\theta < 0$ means a *trans*-shortening and *cis*-elongation, the shortening being twice the elongation (in contrast to the previous cases for which the distortion by ligand substitution with $\Delta\alpha > 0$ is *trans*-elongation). This distortion results in a compressed octahedron with one shorter axis $Y-M-X_{trans}$. Such a *trans*-shortening may be regarded as a *cis*-elongation. Therefore this kind of ligand mutual influence is often called *cis*-influence. Owing to the additivity of the vibronic effects, the substitution of two ligands in *trans*-positions, $MX_6 - \rightarrow MX_4Y_2$, doubles this effect.

Cis-influence of this kind is indeed observed experimentally in octahedral coordination compounds of non-transition elements from the left-hand side of the Periodic Table. Typical examples are provided by the systems *trans*-$SnX_4(CH_3)_2$ with X = F, Cl, Br, NCS,[81] as well as by other Sn(IV) and Ga(III) compounds.

For the second class of (iii) compounds with post-transition elements from the right-hand side of the Periodic Table which have sufficiently low ns AO, F may become negative and the sign of the Q_θ distortion is inverted, $Q_\theta > 0$, which means *trans*-elongation and *cis*-shortening. Though qualitative, the trend in which *trans*-shortening (*cis*-elongation) changes to *trans*-elongation (*cis*-shortening) when passing from left to right in the series of post-transition elements (more precisely, from higher to lower ns orbital energy positions) seems to be true.

In particular, it predicts that for some elements between the above two limits the mutual influence is small to zero. Indeed, in SF_5Cl both the *cis* and *trans* S–F bonds have practically the same lengths as the S–F bond in SF_6.[82] Similarly, there are no changes in bond lengths in $SF_5(NCO)$, $SeF_5(NCO)$, and $TeF_5(NCO)$.[83] In contrast to these results, in IOF_5 the *trans* I–F bond is significantly longer than the *cis* one[84] (see also.[75,76])

For square-planar σ complexes of the type MX_4 the typical HOMO and LUMO, as well as the coordinates of distortion for two types of systems, (i) and (ii), are given in Table 11:

(i) M is a transition metal, and there are eight valence electrons on the σ MO (typical example $[Pt^{II}X_4]$);

(ii) M is a post-transition element in a low oxidation state (typical example $[Te^{II}X_4]$).

A procedure quite similar to that used above for octahedral complexes yields[75,76] for $\Delta\alpha > 0$ in the case (i) $F > O$, $h < 0$, while in the case (ii) $F < 0$, $h > 0$, but in both cases $Fh < 0$, and hence the coordinate of distortion $Q_x < 0$ which means *trans*-elongation. This is the typical *trans*-influence well known for square-planar complexes, in particular, for Pt(II).

The HOMO-LUMO approximation employed above is certainly restricting. If there are several relatively close-in-energy excited states with different symmetries, this approximation may be invalid. Indeed, as shown above, the symmetry of the excited state (together with that of the ground state) determines the coordinate of distortion, and if only one of the active excited states is taken into account, the real distortion may be lost. For instance, if in the σ-bonded octahedral complexes of post-transition elements in higher oxidation states (type (iii)) one goes beyond the HOMO-LUMO approximation and takes into account the vibronic coupling with the next excited electronic state, say t_{1u} (instead of the excited state a_{1g} employed in Table 11), then the coordinate of distortion can be T_{1u}, say, $Q_z' = (1/2)(Z_1 + Z_2 + Z_4 + Z_5)$, which changes the angles between the bonds.[75–77] Further consideration of the vibronic mutual influence of ligands on bond angles have been published.[77]

The HOMO-LUMO approximation is also not appropriate when multiple bonds are taken into consideration because they create more close-in-energy excited states of comparable energy. However, owing to their additive properties, the vibronic contributions can be considered separately for each active excited state; the final result equals the sum of all these contributions (the distortions should be summed up as vectors). This treatment requires more parameters.

If the ligands produce π bonds, they enhance the *trans*-influence, but the sign depends significantly on the coordination center M. Interesting examples of this kind are provided by actinides, where the participation of *f* electrons in the bonding is important. In complexes of the type MX_6 where M is an actinide, HOMO t_{1u} contains both σ and π bonding (s + π bonds), while the LUMO is T_{2u}* (a π MO). The coordinate of distortion for the $MX_6 \rightarrow MX_5Y$ substitution is Q_θ, and its sign

proved to be negative,[75,76] $Q_\theta < 0$. This means that, similar to some post-transition (iii) compounds, the distortion is *trans*-shortening and *cis*-elongating. The experimental data (Table 12) confirm this prediction. Note that in quite similar complexes of transition metals the mutual influence of ligands results in *trans*-elongation. For instance,[85] in $K_2[MoOCl_5]$ (I) and $K_2[ReOCl_5]$ (II) $R(M\text{-}X_{trans})$ is significantly larger than $R(M\text{-}X_{cis})$(in Å): 2.587 and 2.39 in (I) and 2.47 and 2.39 in (II), respectively. This illustrates the fact that the electronic structure of the coordination element M that transfers the mutual influence is important.

9. CONCLUDING REMARKS

The main conclusion which can be made from the results outlined in this paper is that the concept of vibronic interactions may serve as a general tool to the solution of various problems of stereochemistry, including transition metal stereochemistry and crystal chemistry. It is a model approach which starts with a high-symmetry reference configuration and, by means of perturbation theory, predicts how electrons control molecular configurations.

The advantages of this approach, as compared with the existing, mainly semiclassical methods, are that it is devoid of the corresponding limitations with regard to the electronic structure; it can handle non-regular and non-adiabatic systems, non-rigid molecules and systems with internal rotations, as well as crystal structures and structural phase transitions. As compared with full computations with geometry optimization, the vibronic approach is more general, it does not have the 'non-transferability' features of the computer experiments mentioned in the introduction to this paper.

The crystal aspect of the problem is of special importance to many transition metal compounds which are stable in the crystal state only. Vibronic theory allows for a separation of the long-range (cooperative) forces from the local (chemical) ones. Based on this separation, it has been shown that long-range forces alone cannot produce instability of the high-symmetry lattice structure, and hence the actual distortions are of local origin. This rules out the possibility of pure displacive distortions of the lattice and makes doubtful the very existence of a whole class of displacive phase transitions. According to the vibronic concept, the origin of specific molecular shapes and lattice structures should be sought in the corresponding local ground and excited electronic states, their energies and wavefunctions, which allow for strong vibronic mixing (new covalence bonding) under nuclear displacements.

The limitations of the vibronic approach lie in its perturbation formulation: we assume a high-symmetry reference configuration and predict the strength and

Table 12 Experimental data on *cis*-elongation and *trans*-shortening in some actinide MOX_5 compounds (ref. 75).

Compound	R(M--O) Å	$R(M\text{-}X_{trans})$ Å	$R(M\text{-}X_{cis})$ Å
UCl_6	-	2.47	2.47
$(PPh_4)[UOCl_5]$	1.76	2.43	2.53
$(NEt_4)_2[PaOCl_5]$	1.74	2.42	2.64
$(NEt_4)_2[UOCl_4]$	1.75	-	2.67

possible direction of the instability. If the selected reference configuration is close to the expected one, the predicted instability indicates the expected stereochemistry. But, in general, the knowledge of the direction of instability may not be sufficient to predict the stable configuration. For instance, in the case of the $CuCl_5^{3-}$ polyhedron, discussed in Section 5, the vibronic treatment predicts that the system is unstable with respect ot E″ nuclear displacements that transfer the reference TBP configuration toward a SP one, but it does not determine whether the actual configuration will be exactly SP or something else (in fact it is approximately SP).

Thus, strictly speaking, the vibronic approach allows one to determine which configuration is unstable, rather than which is stable. In principle, one can repeat the vibronic treatment for several (all of the) possible configurations, thus narrowing the variety of possible stable configurations. Again, if the reference configuration is not unstable, *i.e.*, it has a minimum, the vibronic approach cannot answer whether this is an absolute minimum. In other words, the vibronic approach does not allow for a choice between isomers.

Within these limitations, the vibronic approach has very wide applications demonstrated in this paper by considering different kinds of stereochemical problems for transition metal compounds.

The treatment in this paper also shows how to handle stereochemical vibronic problems practically. In particular, numerical estimates of the vibronic contribution to the possible instability of the system in different directions may be very useful, and they are not very difficult; semiempirical computations of the type discussed in Section 5 for comparison of copper and zinc polyhedra in similar crystals take several minutes on workstations.

Note that the majority of the problems considered above by means of the vibronic approach have no explanations in existing stereochemical approaches. This refers first to the problems in which the crystal lattice plays a significant role (displacive lattice distortions, plasticity, distortion isomers, temperature dependent conformers, *etc.*). Neither the semiclassical approaches, nor computerized geometry optimization can be used to address these problems. But even for local stereochemistry the vibronic solution may be unique. For instance, the $ZnCl_5^{3-}$ polyhedron is a closed shell system and hence, from the point of view of semiclassical methods, it should have the high-symmetry TBP configuration. As shown in Section 5, vibronic coupling to the appropriate excited states (which fall out of consideration in the semiclassical models) may cause its A″ distortion observed in the $[Co(NH_3)_6][ZnCl_5]$ crystal.

Taken as a whole, the vibronic approach proved to be a further step in theoretical developments of transition metal stereochemistry.

Acknowledgements

Significant contributions to some of the main work discussed in this review were made by my students and coworkers B.G. Vekhter, V.Z. Polinger, and N.N Gorinchoy, and by J. Gazo, N.N. Kristoffel, A.A. Levin, W.J.A. Maaskant, and Ch. Simmons. I acknowledge also the cooperation and discussions with J.P. Fackler, D. Reinen and H. Bill and the valuable support of R.S. Pearlman.

References

1. F.A. Cotton and G. Wilkinson, *Advanced Inorganic Chemistry: A Comprehensive Text,* 5th Edition (Wiley, New York, 1992).
2. J.K. Burdett, *Molecular Shapes. Theoretical Models of Inorganic Stereochemistry* (Wiley-Interscience, New York, 1980).
3. R.G. Gillespie, *Mokecular Geometry* (Van Nostrand, Reinhold, London, 1972); R.G. Gillespie and I. Hargittai, *The VSEPR Model of Molecular Geometry* (Allyn & Bacon, Internat. Student Edition, Hemmel Hempstead, 1991).
4. *Stereochemistry and Bonding,* In: *Structure and Bonding,* v.71 (Springer, Berlin, 1989).
5. J.E. Fergusson, *Stereochemistry and Bonding in Inorganic Chemistry* (Prentice Hall, Englwood Cliffs, 1974).
6. A.F. Wells, *Structural Inorganic Theory* (Clarendon, Oxford, 1984).
7. D.L. Kepert, *Inorganic Stereochemistry* (Springer, Berlin, 1982).
8. I.B. Bersuker, *The Jähn-Teller Effect and Vibronic Interactions in Modern Chemistry* (Plenum, New York, 1984).
9. I.B. Bersuker, Koord. Khim. **19**, 438 (1993).
10. I.B. Bersuker, *Electronic Structure and Properties of Transition Metal Compounds. Introduction to the Theory,* in press (Russian Editions: Khimiya, Leningrad, 2nd Ed., 1976; 3rd Ed., 1986).
11. G. Fischer, *Vibronic Coupling: The Interaction Between the Electronic and Nuclear Motions* (Academic Press, London, 1984).
12. I.B. Bersuker and V.Z. Polinger, *Vibronic Interactions in Molecules and Crystals, (Springer,* New York, 1989).
13. H.A. Jähn and E. Teller, *Proc. Roy. Soc.* **161**, 220 (1937).
14. R. Englman, *The Jhn-Teller Effect in Molecules and Crystals* (Wiley, New York, 1972).
15. D.M.P. Mingos and L. Zhenyang, *Structure and Bonding* **71**, 1 (1989).
16. D.M.P. Mingos, *Pure & Appl. Chem.* **59**, 145 (1987).
17. R.F.W. Bader, *Mol. Phys.* **3**, 137 (1960); *Canad. J. Chem.* **40,** 1164 (1962); R.F.W. Bader and A.D. Bandrauk, *J.Chem. Phys.* **49,** 1666 (1968).
18. R.G. Pearson, *Symmetry Rules for Chemical Reactions, Orbital Topology and Elementary Processes* (Wiley, New York, 1976).
19. I.B. Bersuker, *Teor. i Eksp. Khim.* **16,** 291 (1980); *Nouv. J. Chim.* **4**, 139 (1980).
20. I.B. Bersuker, N.N. Gorinchoi, and V.Z. Polinger, *Thoret. Chim.Acta* **66**, 161 (1984); *J. Mol. Sruct. (Theochem)* **270,** 369 (1992).
21. I.B. Bersuker, *Fiz. Tverdogo Tela (Sov. Phys. - Solid State)* **30,** 1738 (1988).
22. T.K. Rebane, *Teor. i Eksp. Khim.* **20,** 532 (1984).
23. I.B. Bersuker, *Phys. Lett.* **20**, 589 (1966).
24. I.B. Bersuker and B.G. Vekhter, *Fiz. Tverdogo Tela* (Sov. Phys. - Solid State) **9**, 2652 (1967).
25. I.B. Bersuker, *Ferroelectrics,* 1995, in press.
26. I.B. Bersuker, *New J. Chem.* **17,** 3 (1993).
27. V.Z. Polinger, N.N. Gorinchoy and I. B. Bersuker, *Chem. Phys.* **159,** 75 (1992).
28. I.B. Bersuker and B.G. Vekhter, *Ferroelectrics* **19,** 137 (1978); I.B. Bersuker, in: *The Interband Model of Ferroelectrics,* Ed. E.V. Bursian (Gertsen Pedagogical Institute, Leningrad, 1987) p.8.
29. I.B. Bersuker, B.G. Vekhter, and A.A. Muzalewskii, *Feroelectrics* **6,** 197 (1974).
30. I.B. Bersuker, N.N. Gorinchoy, T.A. Fedorko, *Ferroelectrics,* **155,** 7 (1994).
31. N.N. Kristoffel and P.I. Konsin, in: *Titanat Baria* (Moscow, Nauka, 1973) p.11; *Ferroelectrics* **6,** 3 (1973).
32. P.I. Konsin and N.N. Kristoffel, in: the *Interband Model of Ferroelectrics,* Ed., E.V. Bursian (Gertsen Pedagogical Institute, Leningrad, 1987) p. 32.
33. I.B. Bersuker and B.G. Vekhter, *Izvestia AN SSSR, Ser. Fiz.* **33**, 199 (1969).
34. M.E. Lines and A.M. Glass, *Principles and Applications of Ferroelectrics and Related Materials* (Clarendon Press, Oxford, 1977).
35. M. Lanbert, R. Comes, *Sol. State Commun.* **7**, 305 (1969).
36. R. Comes, M. Lambert, and A. Guinier, *Solid State Commun.* **6,** 715 (1968).
37. K.A. Muller, in: *Nonlinearity in Condensed Matter,* Ed., A.R.Bishop (Springer, Heidelberg, 1986) p. 234.
38. K.H. Ehses, H. Bock, and K. Fischer,*Ferroelectrics* **37,** 507 (1981).
39. K. Itoh, L.Z. Zeng, E. Nakamura, and N. Mishima, *Ferroelectrics* **63,** 29 (1985).

40. O. Hanske-Petitpierre, Y. Yacoby, J. Mustre de Leon, E.A. Stern, and J.J. Rehr, *Phys. Rev.* B **44,** 6700 (1991).
41. T.P. Dougherty, G.P. Wiederrecht, K.A. Nelson, M.H. Garrett, H.P. Jensen, and C. Warde, *Science* **258**, 770 (1992).
42. M.D. Fontana, A. Ridah, G.E. Kugel, and C. Carabatos-Nedelec, *J.Phys.C* **21**, 5853 (1988); *Phys. Rev. B* **40**, 786 (1989).
43. T.P. Dougherty. *Abstracts, Third Williamsburg Workshop on First-Principles Calculations for Ferroelectricity* (Williamsburg, Virginia, 1994).
44. N. Sicron, B. Ravel, Y. Yacoby, E.A. Stern, F. Dogan, and J.J. Rehr, *Phys. Rev. B* (to be published).
45. W.J.A. Maaskant and I.B. Bersuker, *J. Phys. C* **3**, 37 (1991).
46. R.E. Cohen and H. Krakauer, *Phys. Rev. B* **42,** 6416 (1990) .
46. R.E. Cohen and H.Krakauer, *Phys. Rev. B* **42,** 6416 (1990).
47. R.E. Cohen and H. Krakauer, *Ferroelectrics* **136,** 65 (1992).
48. A.M. Quittet, M. Lambert, and A. Guinier, *Sol. State Commun.* **12,** 1053 (1973).
49. G. Burns and F. Dacol, *Ferroelectrics,* **37**, 661 (1981).
50. F. Gervais, *Ferroelectrics* **53,** 91 (1984).
51. D.W. Meek and J.A. Ibers, *Inorg. Chem.* **9**, 405 (1970).
52. D. Reinen and C. Friebel, *Inorg. Chem.***23,** 792 (1984).
53. D. Reinen and M. Atanasov, *Chem. Phys.*136, 27 (1989); **155**, 157 (1991).
54. M. Atanasov, W. Koenig, M. Craubuner and D. Reinen, *New J. Chem,* **17,** 115 (1993).
55. N.N. Gorinchoy, I.B. Bersuker and V.Z. Polinger,*New J. Chem.* **17,** 125 (1993).
56. J. Gazo, I.B. Bersuker, J. Garaj, M. Kabesova, J. Kohout, H. Langfelderova, M. Melnik and M. Serator F. Valach, *Coord. Chem. Rev.* **19,** 253 (1976).
57. Ch. J. Simmons, *New. J. Chem.* **17,** 77 (1993).
58. I.B. Bersuker, *Zh. Struct. Khim.* **16,** 935 (1975).
59. B.J. Hathaway, *Structure and Bonding* **57**, 55 (1984).
60. J. Pradilla-Sorzano and J.P. Fackler, *Inorg. Chem.* **12,** 1182 (1973).
61. J.P. Fackler and A. Avdeev, *Inorg. Chem.* **13,** 1864 (1974).
62. J. Gazo, *Pure and Appl. Chem.* **38,** 279 (1974).
63. C. Friebel and D. Reinen, *Zs. Anorg. Allgem. Chem.* **407,** 193 (1974).
64. J.K. Burdett, *Inorg. Chem.* **20,** 1959 (1981).
65. B. Papankova, M. Serator, J. Strachelsky and J. Gazo, *Proc. 8the Conf. Coord. Chem.* (Smolenice, Bratislava, 1980) p. 321.
66. T. Obert and I.B. Bersuker, *Proc. XIX ICCC,* v. 2 (Prague, 1978) p.94; *Czechosl. J. Phys. B,* **33,** 568 (1983).
67. L.E. Orgel, *J. Chem. Educ.* 3815 (1959).
68. S.Y. Wang and L.L. Lohr, Jr., *J. Chem. Phys.* **60,** 3901 (1974); **61,** 4110 (1974).
69. W.J.A. Maaskant and Il.B. Bersuker, *J. Phys. C: Condensed Matter* **3,** 37 (1991).
70. L.S. Bartel and R.M. Gavin, *J. Chem. Phys.* **48,** 2466 (1968).
71. M.R. Mingos, *Introduction to Cluster Chemistry* (Prentince Hall, Hertfordshire, 1990).
72. W.J.A. Maaskant, *New J. Chem.* **17**, 97 (1993).
73. A. Ceulemans, *J. Chem. Phys.* **84,** 6442 (1986).
74. A. Ceulemans, L.G. Vanquickenborne, *The Expikernel Principle,* In: *Structure and Bonding,* v.71 (Springer, Berlin, 1989) p. 125.
75. A.A. Levin, In: *Sov. Sci. Rev. B., Chem. Rev.* **9**, 279 (1987).
76. A.A. Levin and P.N. Dyachkov, *Electronic Structure, Geometry, Isomerism and Transformations of Heteroligand Molecules (Russ.)* (Nauka, Moscow, 1990).
77. A.A. Levin, *New J. Chem.* **17,** 31 (1993).
78. F.R. Hartley, *Chem. Soc. Rev.* **2,** 163 (1973).
79. E.M. Shustorovich, M.A. Porai-Koshitz and Iu.A. Buslaev, *Coord. Chem. Rev.* **17,** 1 (1975).
80. V.I. Nefedov and M.M. Hofman, *Mutual Influence of Ligands in Inorganic Compounds (Russ.),* In: Itoghi Nauki i Techniki, Ser. *Inorganic Chemistry,* v.6 (VINITI, Moscow, 1978).
81. C.W. Hobbs and R.S. Tobias, *Inorg. Chem.* **9**, 1037 (1970).
82. L.S. Bartell, S. Doun and C.J. Marsden, *J. Mol. Struct.* **75,** 271 (1981).
83. H. Oberhammer, K. Seppelt and R. Mews, *J. Mol. Struct* **101,** 325 (1983).
84. L.S. Bartell, F.B. Clippard and E.J. Jacob, *Inorg. Chem.* **15,** 3009 (1976).
85. M.A. Porai-Koshitz and L.A. Atovmean, *Crystal Chemistry and Stereochemistry of Molybdenum Coordination Compounds (Russ.)* (Nauka, Moscow, 1974).